NASA TECHNICAL NOTE

NASA TN D-2328

NASA TN D-2328

COMPARISON OF THE HYPERSONIC AERODYNAMIC CHARACTERISTICS OF SOME SIMPLE WINGED SHAPES IN AIR AND HELIUM

by Thomas A. Blackstock and Charles L. Ladson

Langley Research Center
Langley Station, Hampton, Va.

NATIONAL AERONAUTICS AND SPACE ADMINISTRATION • WASHINGTON, D. C. • JUNE 1964

COMPARISON OF THE HYPERSONIC AERODYNAMIC CHARACTERISTICS OF SOME SIMPLE WINGED SHAPES IN AIR AND HELIUM

By Thomas A. Blackstock and Charles L. Ladson

Langley Research Center
Langley Station, Hampton, Va.

NATIONAL AERONAUTICS AND SPACE ADMINISTRATION

For sale by the Office of Technical Services, Department of Commerce,
Washington, D.C. 20230 -- Price $1.00

COMPARISON OF THE HYPERSONIC AERODYNAMIC CHARACTERISTICS OF SOME SIMPLE WINGED SHAPES IN AIR AND HELIUM

By Thomas A. Blackstock and Charles L. Ladson
Langley Research Center

SUMMARY

An investigation was made in the Langley 11-inch hypersonic tunnel at Mach numbers of 6.8 and 9.6 in air and 10.9 and 18.0 in helium to determine the force and moment characteristics of a series of wings. This investigation was made to study the simulation of high Mach number aerodynamics in air by the use of helium as a test medium. The wings tested were of both square and delta planform and included both sharp and blunt leading edges. Also the effects of a vertical forward-facing step on the characteristics of the square wing were investigated. The angle-of-attack range for the tests was from 0° to 25°.

Analysis of the results indicated that lift and drag coefficients could be predicted over the range of test Mach numbers and for the test media used. Drag coefficients could not be as adequately predicted as lift coefficients due to viscous effects. Good simulation was obtained for normal-force coefficients, however. The forward-facing step on the square wing produced a large increase in lift and pitching-moment coefficients and may be used as a pitch control device. Two methods of correlating normal-force coefficients are also presented.

INTRODUCTION

In addition to its use for basic fluid-dynamics studies, the use of helium as a test medium for the simulation of aerodynamic characteristics has received considerable attention in theoretical work. (See refs. 1, 2, and 3.) Experimental verification of these theories is necessary to establish fully the validity of helium tests for this purpose. (See refs. 4 to 7.) The present paper presents data on some simple winged shapes for which aerodynamic characteristics can be readily calculated.

The purpose of this paper is to compare the force and moment coefficients for a series of wings tested at Mach numbers of 6.8 and 9.6 in air and 10.9 and 18.0 in helium. The models were tested at angles of attack up to 25° in air and 15° in helium. The effects of Mach number and test medium are presented and compared with theoretical estimates. Two methods for correlating normal-force coefficients are also discussed. Some of the present data along with additional data on these models at other Mach numbers have been published in reference 6.

SYMBOLS

c	root chord
C_A	axial-force coefficient, $\frac{\text{Axial force}}{qS}$
C_D	drag coefficient, $\frac{\text{Drag}}{qS}$
C_L	lift coefficient, $\frac{\text{Lift}}{qS}$
C_m	pitching-moment coefficient, $\frac{\text{Pitching moment}}{qSc}$
C_N	normal-force coefficient, $\frac{\text{Normal force}}{qS}$
$C_N' = C_{N,H} \frac{\gamma_A + 1}{\gamma_H + 1}$	
L/D	lift-drag ratio
M	Mach number
q	dynamic pressure
R	Reynolds number
S	planform area
α	angle of attack, measured from lower surface of model
γ	ratio of specific heats of gas
Λ	sweep angle

Subscripts:

A	in air
H	in helium

APPARATUS, MODELS, AND TESTS

All data were obtained in the Langley 11-inch hypersonic tunnel at Mach numbers of 6.8 and 9.6 in air and 10.9 and 18.0 in helium. A calibration of

the Mach number 6.8 nozzle is given in reference 8 and a calibration for the Mach number 9.6 nozzle is shown in reference 9. A description and calibration of the two helium nozzles are presented in the appendix of reference 5.

The models tested are shown in figure 1 and were machined from stainless steel. The forces and moments were measured on an external strain-gage balance with angles of attack set optically by use of a light beam reflected from the model onto a calibrated scale. This method gave the true angle of attack of the model. Angle of attack was measured from the lower surface of the models. The moment reference was located at the centroid of area in plan view for all models, at one-third of the vertical height in side view for the delta wings, and at one-half the vertical height in side view for the square wing.

The maximum estimated errors for the force and moment data on the square-planform wing based on the balance inaccuracy is presented in the following table:

M	C_N	C_A	C_m
6.8	0.0086	0.0026	0.0131
9.6	.0088	.0027	.0134
10.9	.0037	.0011	.0057
18.0	.0050	.0015	.0076

Over the range of test conditions for each Mach number, the ratio of specific heats was constant. The test Reynolds numbers for the various configurations are presented in the following table and are based on free-stream conditions and root chord of the model:

Model	R at -			
	M = 6.8	M = 9.6	M = 10.9	M = 18.0
$\Lambda = 0^\circ$ wing	0.33×10^6	0.33×10^6	1.29×10^6	1.45×10^6
$\Lambda = 60^\circ$ wing	.35	.35	1.36	1.54
$\Lambda = 70^\circ$ wing	.55	.55	2.15	2.42

RESULTS AND DISCUSSION

Theoretical Predictions

The theoretical estimates of normal- and axial-force coefficients (therefore, lift, drag, and lift-drag ratio) were determined from combinations of oblique-shock theory, modified Newtonian theory, and skin friction. Oblique-shock theory has been used to compute pressure forces on the plane surfaces of the models, including cases where the leading edges were blunted. In computing normal-force coefficients by Newtonian theory the maximum pressure coefficient

used is that referred to in reference 2 as the flat-plate modified Newtonian coefficient, $C_{p,max} = \gamma + 1$. For the models with the blunt leading edges, Newtonian theory as presented in reference 11 was used to determine the force coefficient of the leading edge. The maximum pressure coefficient used is that referred to as the blunt-nose modified Newtonian theory in reference 2 and is given by $C_{p,max} = \frac{\gamma + 3}{\gamma + 1}$.

The skin-friction calculations include boundary-layer displacement effects. These calculations were made only at zero angle of attack because the theoretical variation with angle of attack is small. The skin friction for the square-planform wings was computed by the method outlined in appendix A of reference 12, whereas the skin friction for the delta wings was computed by strip theory as shown in appendix C of reference 9. Local conditions just outside the boundary layer were used and the boundary layer was assumed to be laminar.

For the theoretical estimates of the forces on the models with the forward-facing step, boundary-layer separation was assumed to start at the leading edge. It was further assumed that the separated region was wedge shaped with its height at the trailing edge being equal to the height of the step. In the computation of incremental forces by this method, the selection of the separation point location is not critical. The variation in incremental lift coefficient obtained with the separation point located at the leading edge and at 75 percent chord was less than 2 percent for the model tested at an angle of attack of 25°.

Experimental Results

Stability-axis data.- Experimental values of lift and drag coefficients and lift-drag ratio are presented in figure 2 and compared with theory. The inviscid theory shown includes only the pressure forces on the models as determined from oblique-shock theory for the plane surface and modified Newtonian theory for the blunt leading edges.

Lift coefficients in both air and helium are very well predicted by the inviscid theory in almost all cases. Drag coefficient and lift-drag ratio were also in good agreement with calculations for the sharp-leading-edge configurations in air when skin friction was added to the inviscid theory; however, drag coefficient was often underestimated and, thus, the predicted lift-drag ratios exceeded the experimental values. Although base drag has not been taken into account, its effect is small.

The effect of planform shape on lift and drag is secondary for the sharp-leading-edge models in that its main effect is to vary the local angle of attack of the upper wing surface. This effect manifests itself in a reduced drag at angles of attack below 11° for wings of increasing sweep angle as can be seen in figures 2(c) and 2(d). Above this angle the top surface is shielded from the flow and the computed normal force and skin friction are independent of planform. The negative lift contribution of the upper surface at low angles of attack is also reduced as the sweep angle is increased. On the wings with

the blunt leading edges there is a more pronounced effect of planform shape, since the leading-edge drag decreases markedly with increasing sweepback angle. This effect is best illustrated by the maximum lift-drag ratio at a Mach number of 6.8 which increases from 2 to 3 as the sweepback angle is increased from 0° to 70°. (See figs. 2(e), 2(g), and 2(h).) The effect of the forward-facing step on the characteristics of the square planform wing should be noted. As can be seen in figures 2(b) and 2(f), increases of 10 to 20 percent in lift coefficient along with increases in drag coefficient of up to 30 percent were produced.

In figure 3, pitching-moment coefficients plotted against angle of attack are presented. Pitching-moment coefficients for air and helium are essentially the same. As would be expected, the pitching-moment coefficients are approximately zero except for the models with the forward-facing step. A maximum shift in the center-of-pressure location of about 6 percent for this model is indicated. The pitching-moment contribution of the step is sizable in view of its small area, and the step may be used as a pitch control device.

Body-axis data.- In figure 4 experimental values of normal-force coefficients are presented and compared with oblique-shock ("exact") theory and modified Newtonian theory. As for lift coefficient, the oblique-shock theory usually gives quite accurate predictions of normal-force coefficient. The data from modified Newtonian theory also are in fair agreement with the experimental data and, as expected, is in best agreement with the data for higher Mach numbers. In general it is also in better agreement with the data on the blunt-leading-edge models.

In figure 5 axial-force coefficient is compared with exact theory, a combination of oblique-shock theory for flat surface, Newtonian theory for the blunt leading edges, and skin-friction coefficient. In general, the theory predicts trends in the force variation with angle of attack but fails to predict the magnitude of the force. Agreement between experiment and theory is generally better at the higher Mach numbers for both air and helium. Above 11° angle of attack, the theoretical axial force is purely skin friction on the sharp-leading-edge models without the step. At Mach numbers of about 10, agreement between theory and experiment is better in air than in helium. This difference may be the result of boundary-layer transition on the models at the higher Reynolds numbers of the helium tests. It can be seen that for the tests made in air the axial force is higher at low angles of attack for $M = 6.8$ and higher at high angles of attack for $M = 9.6$, with the crossover point usually around 12°. This effect is due to the higher pressure forces at $M = 6.8$ at the lower angles of attack. These pressure forces diminish with increasing angle of attack until the higher skin friction of the tests at $M = 9.6$ becomes dominant. In figures 5(g) and (h) it is seen that the theoretical axial-force coefficient increases with angle of attack above 12°. This increase is due to a decrease in the effective sweep angle with increasing angle of attack. This effect overshadows the increasing amount of leading edge which is shielded from the flow and would thus tend to decrease the leading-edge contribution.

Normal-force correlation.- In figure 6, a simple correlation of normal-force coefficients has been made based on the flat-plate modified Newtonian theory. Data from the tests at Mach number 9.6 (air) and 10.9 (helium) have

been used in an attempt to minimize any Mach number effects. Normal-force coefficients shown on the left of each figure illustrate the effects of the variation in the ratio of specific heats. The correlated normal-force coefficients, C_N' and $C_{N,A}$ presented on the right show the effect of multiplying the normal-force coefficients obtained in helium by $\frac{\gamma_A + 1}{\gamma_H + 1}$. The data are well correlated by this parameter and there is no noticeable effect of leading-edge blunting or sweep angle.

In figure 7 the normal-force coefficients have been correlated on the basis of parameters suggested by the work of Linnell (ref. 10). These parameters and also the theoretical curves shown are taken from his equation,

$$\frac{C_N}{\alpha^2} = \frac{\gamma + 1}{2} + \sqrt{\left(\frac{\gamma + 1}{2}\right)^2 + \frac{4}{(M\alpha)^2}} + \frac{2}{\gamma(M\alpha)^2}\left[1 - \left(1 - \frac{\gamma - 1}{2} M\alpha\right)\frac{2\gamma}{\gamma - 1}\right] \qquad (1)$$

which is written in the nomenclature of this paper. Equation (1) can be reduced to the form

$$C_N M^2 = (M \sin \alpha)^2\left[\frac{\gamma + 1}{2} + \sqrt{\left(\frac{\gamma + 1}{2}\right)^2 + \frac{4}{(M\alpha)^2}}\right] \qquad (2)$$

when the term $\frac{2}{\gamma(M\alpha)^2}\left[1 - \left(1 - \frac{\gamma - 1}{2} M\alpha\right)\frac{2\gamma}{\gamma - 1}\right]$ approaches zero.

Since this equation is strictly applicable only to flat plates, no experimental data are presented for the lower angles of attack. Although the equation may be of value for shapes other than a flat plate, it can not be used in its present form whenever negative lift occurs at positive angles of attack.

The parameters used give good correlation and equation (2) gives a fair prediction of the data. It should be noted, however, that the theory for air is in closer agreement with the data in most cases.

CONCLUDING REMARKS

An investigation was made in the Langley 11-inch hypersonic tunnel at Mach numbers of 6.8 and 9.6 in air and 10.9 and 18.0 in helium to determine the force and moment characteristics of a series of wings. The wings tested were of both square and delta planform and included both sharp and blunt leading edges. The effects of a vertical forward-facing step on the characteristics of the square

wing are also investigated. The angle-of-attack range for these tests was from 0° to 25°.

Analysis of the results indicates that lift, drag, and normal-force coefficients can be adequately predicted over the range of test Mach numbers and the test media used. Drag coefficients could not be as accurately predicted as lift coefficients due to viscous effects. Excellent agreement of experiments in air and helium with oblique-shock theory clearly establishes the validity of helium simulation for lift and normal-force studies where pressure forces are dominant. The forward-facing step on the square wing produced a large increase in lift coefficient and pitching moment and may be used as a pitch control device. Two methods of correlating normal-force coefficients are also presented. One method, based on Newtonian theory, can be used to correlate normal-force coefficients in air and helium at approximately the same Mach number. The other method used also gave good correlation and takes Mach number effects into account. This method may also be used to predict normal-force coefficient.

Langley Research Center,
National Aeronautics and Space Administration,
Langley Station, Hampton, Va., February 29, 1964.

REFERENCES

1. Mueller, James N.: Conversion of Inviscid Normal-Force Coefficients in Helium to Equivalent Coefficients in Air for Simple Shapes at Hypersonic Speeds. NACA TN 3807, 1956.

2. Love, Eugene S., Henderson, Arthur, Jr., and Bertram, Mitchel H.: Some Aspects of Air-Helium Simulation and Hypersonic Approximations. NASA TN D-49, 1959.

3. Bertram, Mitchel H., and Blackstock, Thomas A.: Some Simple Solutions to the Problem of Predicting Boundary-Layer Self-Induced Pressures. NASA TN D-798, 1961.

4. Ladson, Charles L.: A Comparison of Aerodynamic Data Obtained in Air and Helium in the Langley 11-Inch Hypersonic Tunnel. NASA TM X-666, 1962.

5. Ladson, Charles L., and Blackstock, Thomas A. (With appendix by Donald L. Baradell and Thomas A. Blackstock): Air-Helium Simulation of the Aerodynamic Force Coefficients of Cones at Hypersonic Speeds. NASA TN D-1473, 1962.

6. Henderson, Arthur, Jr.: Experimental Investigation of the Air-Helium Simulation Problem on Various General and Specific Configurations at Hypersonic Speeds. Presented at Second Nat. Symposium on Hypervelocity Techniques (Univ. of Denver), Mar. 1962.

7. Arrington, James P., and Maddalon, Dal V.: Aerodynamic Characteristics of Several Lifting and Nonlifting Configurations at Hypersonic Speeds in Air and Helium. NASA TM X-918, 1964.

8. Bertram, Mitchel H.: Exploratory Investigation of Boundary-layer Transition on a Hollow Cylinder at a Mach Number of 6.9. NACA Rep. 1313, 1957. (Supersedes NACA TN 3546.)

9. Bertram, Mitchel H.: Boundary-Layer Displacement Effects in Air at Mach Numbers of 6.8 and 9.6. NASA TR R-22, 1959. (Supersedes NACA TN 4133.)

10. Linnell, Richard D.: Two-Dimensional Airfoils in Hypersonic Flow. Jour. Aero. Sci., vol. 16, no. 1, Jan. 1949, pp. 22-30.

11. Malvestuto, Frank S., Jr., Sullivan, Phillip J., Marcy, William L., Mortzschky, Herbert A., Larrivee, Jules A., and Huggins, Vivan E.: Study To Determine Aerodynamic Characteristics on Hypersonic Re-Entry Configurations. Part II - Analytical Phase, Volume 2 - Design Charts. WADD-TR-61-56, Pt. II, Vol. 2 (AD 28 6890), U.S. Air Force, Aug. 1962.

12. Bertram, Mitchel H., and Feller, William V.: A Simple Method for Determining Heat Transfer, Skin Friction, and Boundary-Layer Thickness for Hypersonic Laminar Boundary-Layer Flows in a Pressure Gradient. NASA MEMO 5-24-59L, 1959.

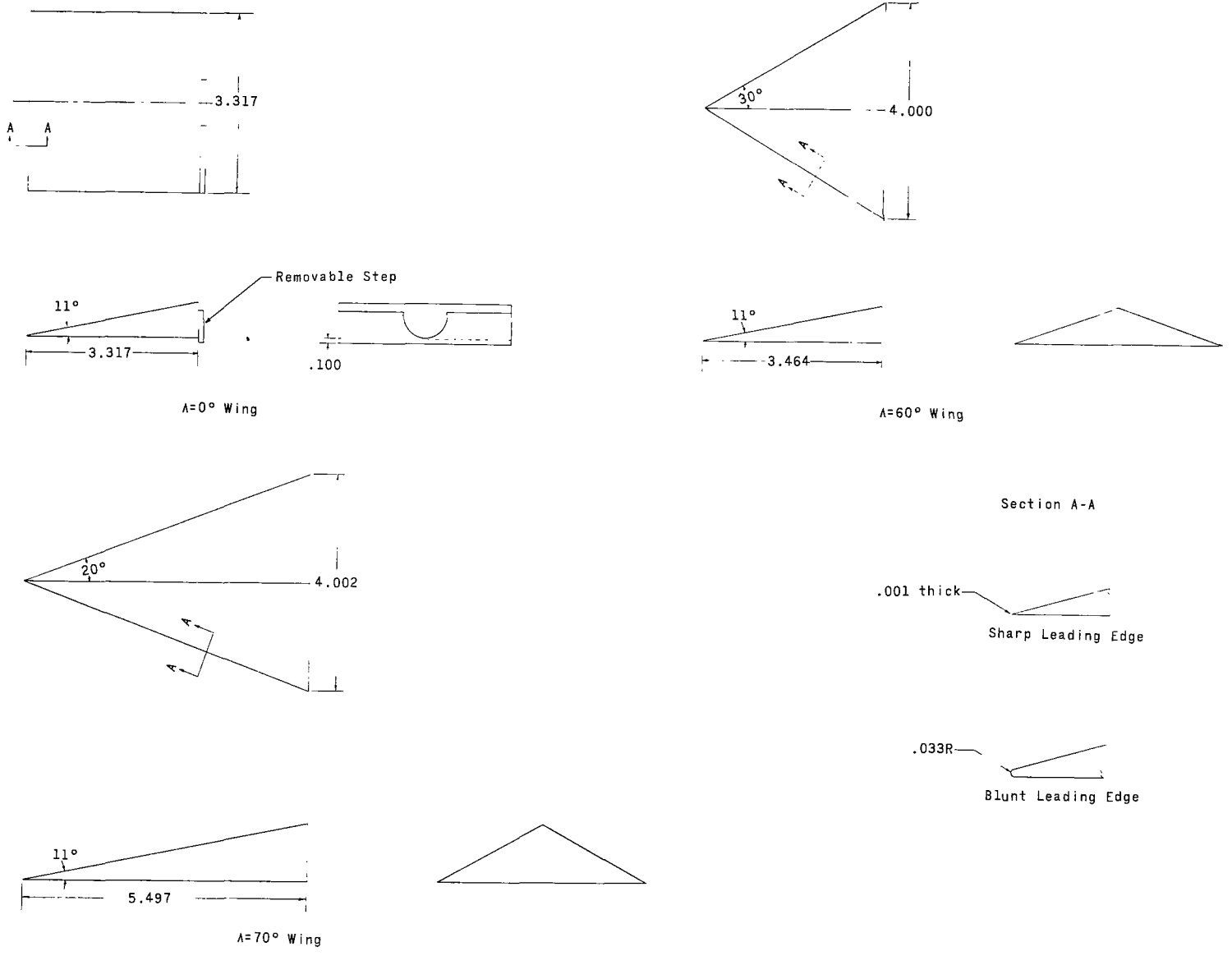

Figure 1.- Model drawings and dimensions. All linear dimensions are in inches.

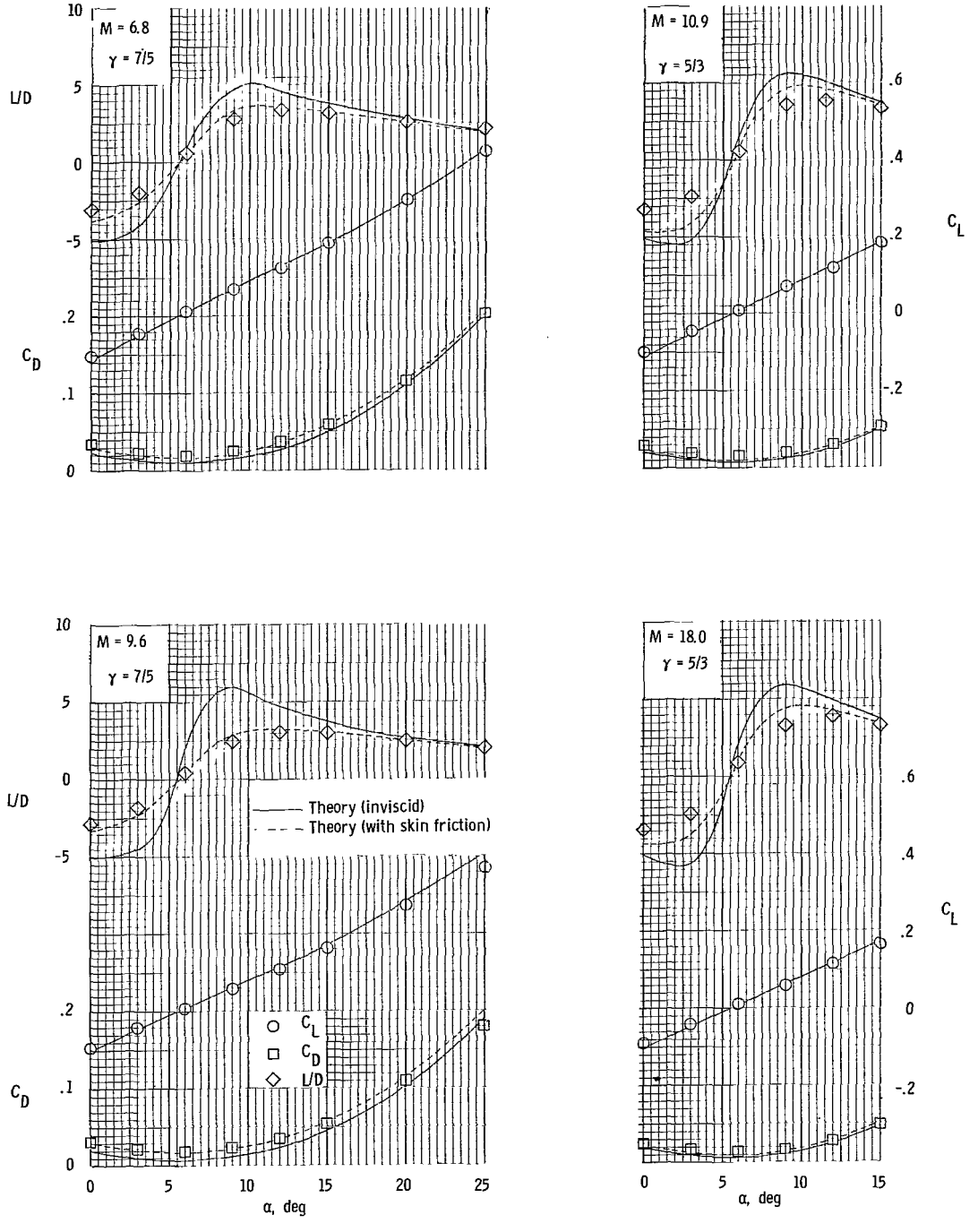

(a) $\Lambda = 0^{\circ}$ wing with sharp leading edge.

Figure 2.- A comparison of experimental lift and drag coefficients and lift-drag ratio with theory for the various wings.

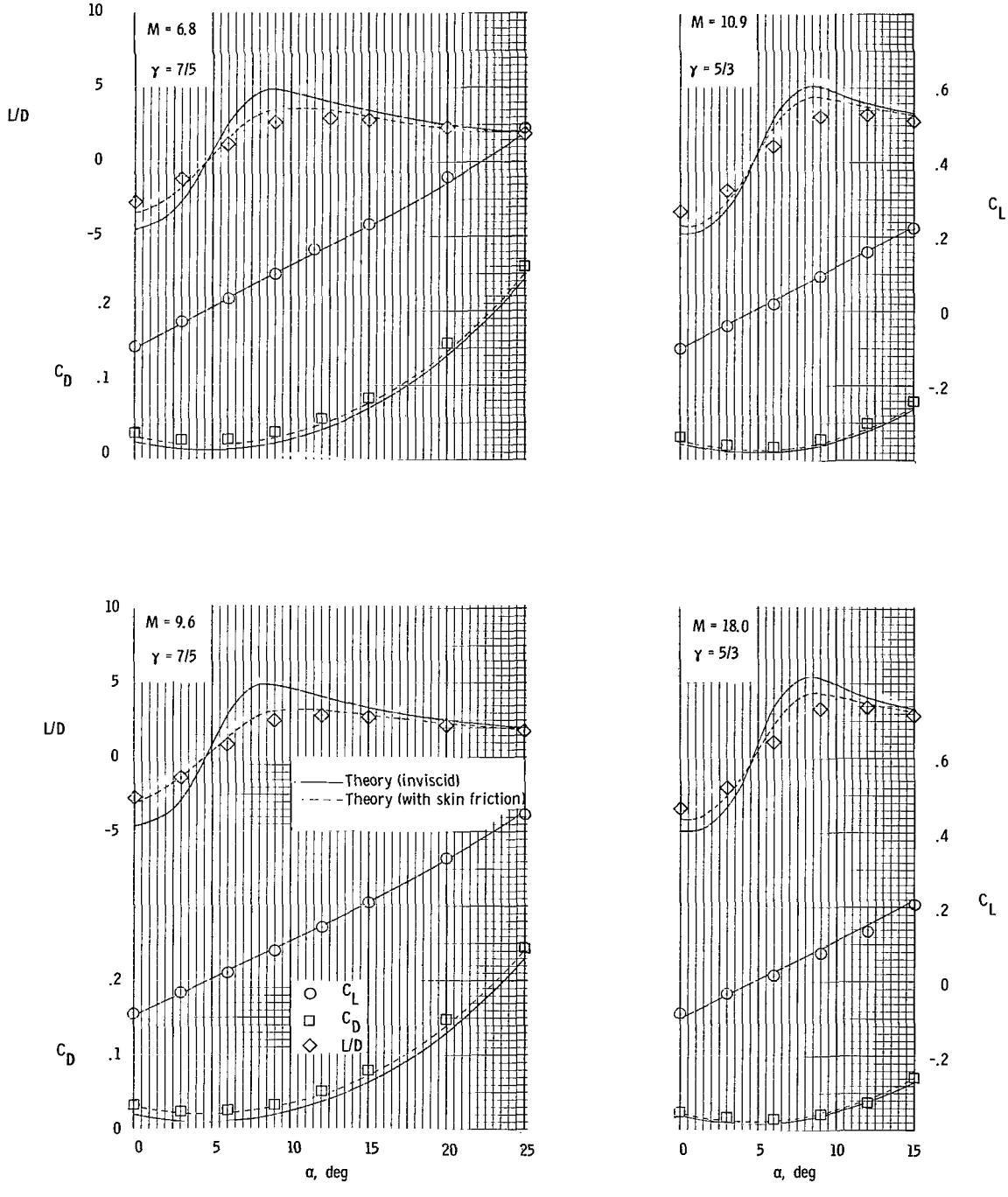

(b) $\Lambda = 0^{\circ}$ wing with sharp leading edge and forward-facing step.

Figure 2.- Continued.

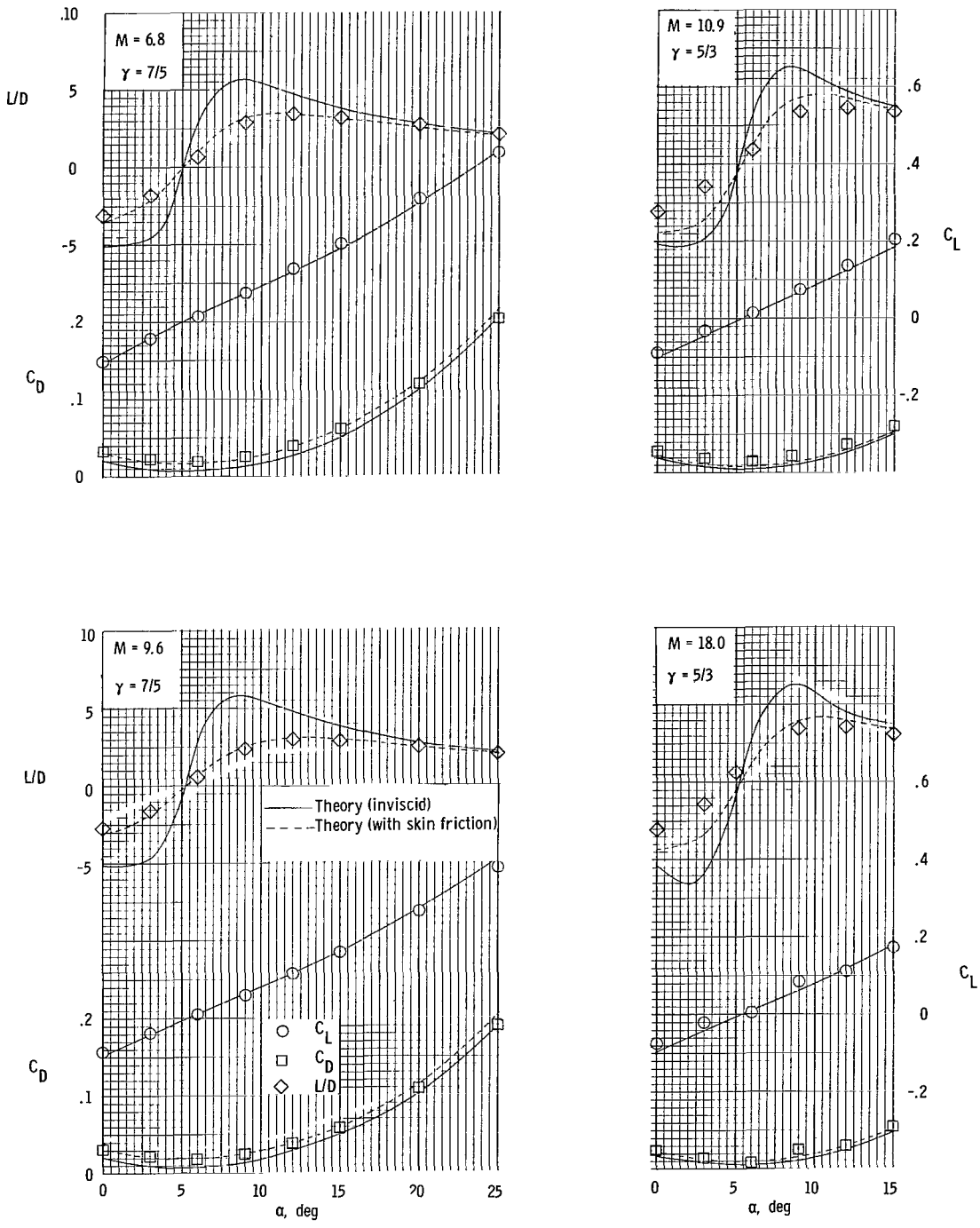

(c) $\Lambda = 60^{\circ}$ wing with sharp leading edge.

Figure 2.- Continued.

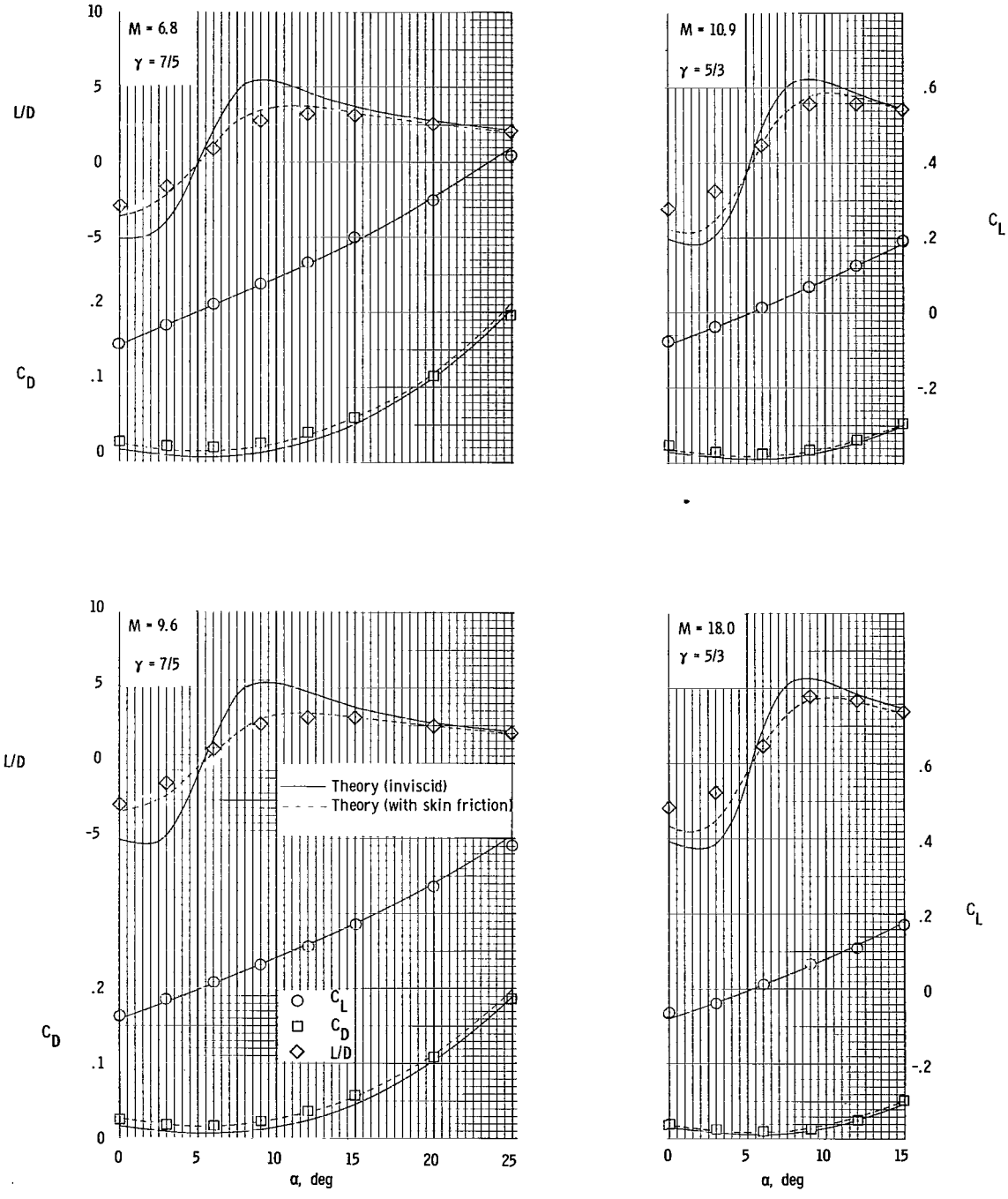

(d) $\Lambda = 70^{\circ}$ wing with sharp leading edge.

Figure 2.- Continued.

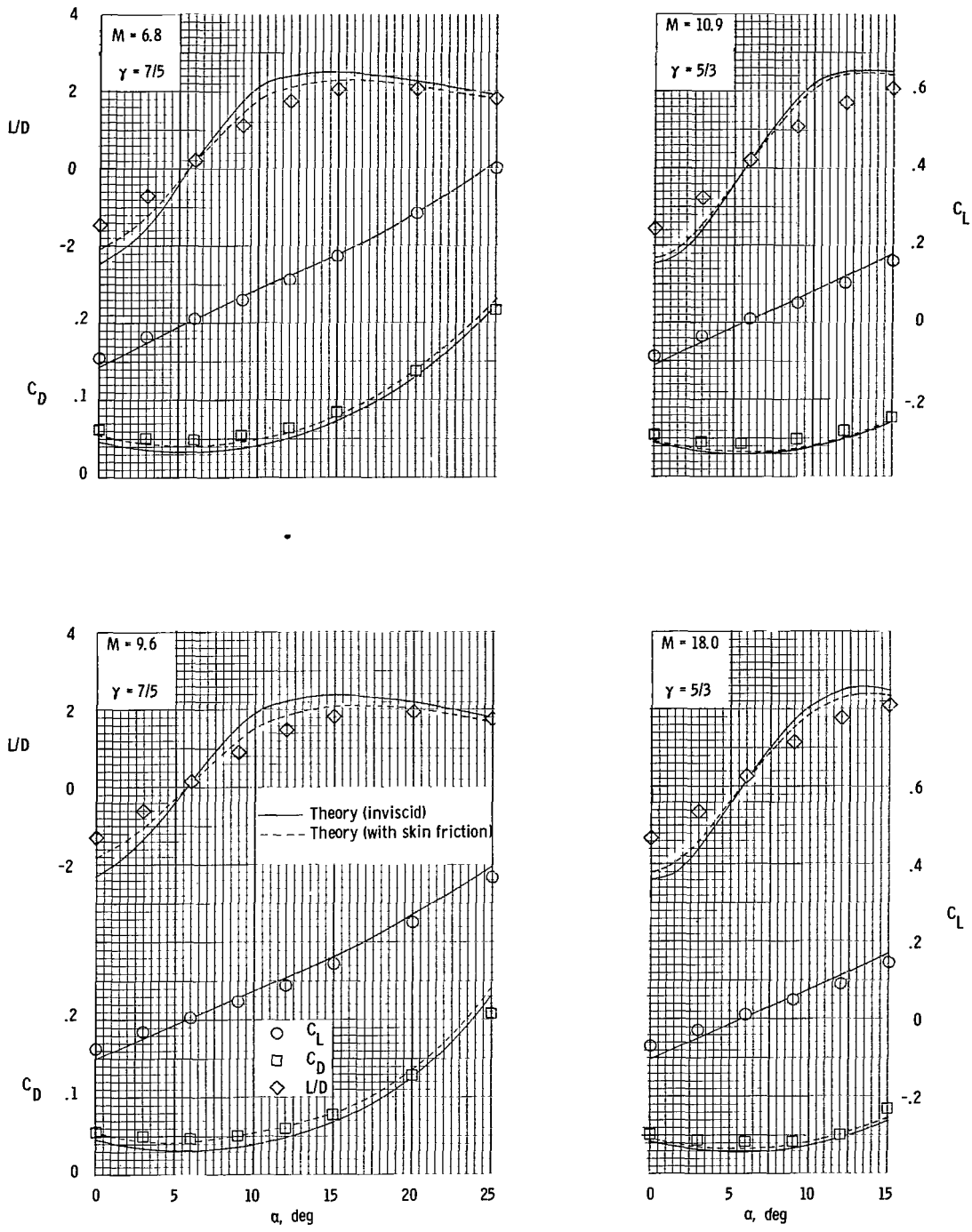

(e) $\Lambda = 0^{\circ}$ wing with blunt leading edge.

Figure 2.- Continued.

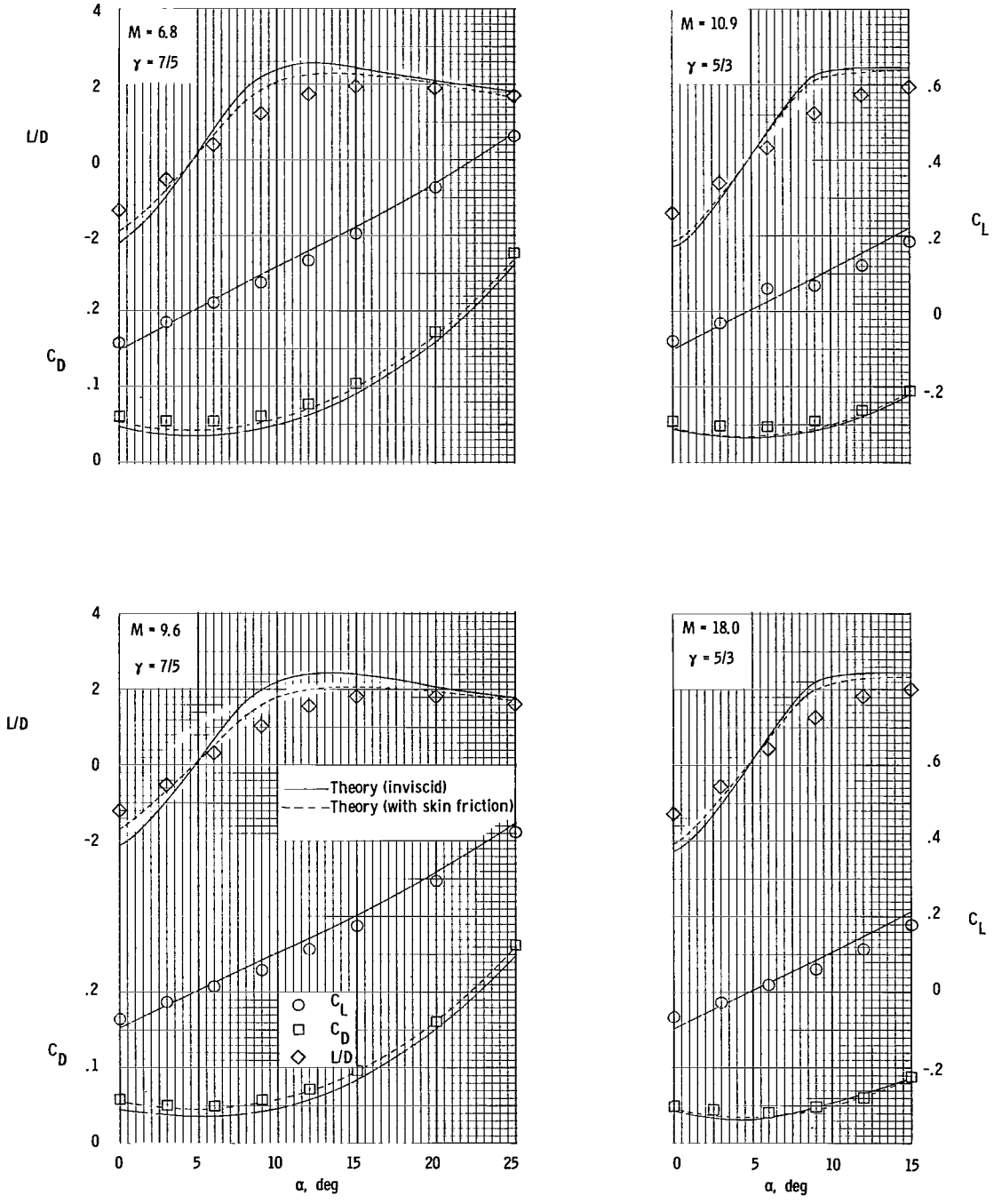

(f) $\Lambda = 0^\circ$ wing with blunt leading edge and forward-facing step.

Figure 2.- Continued.

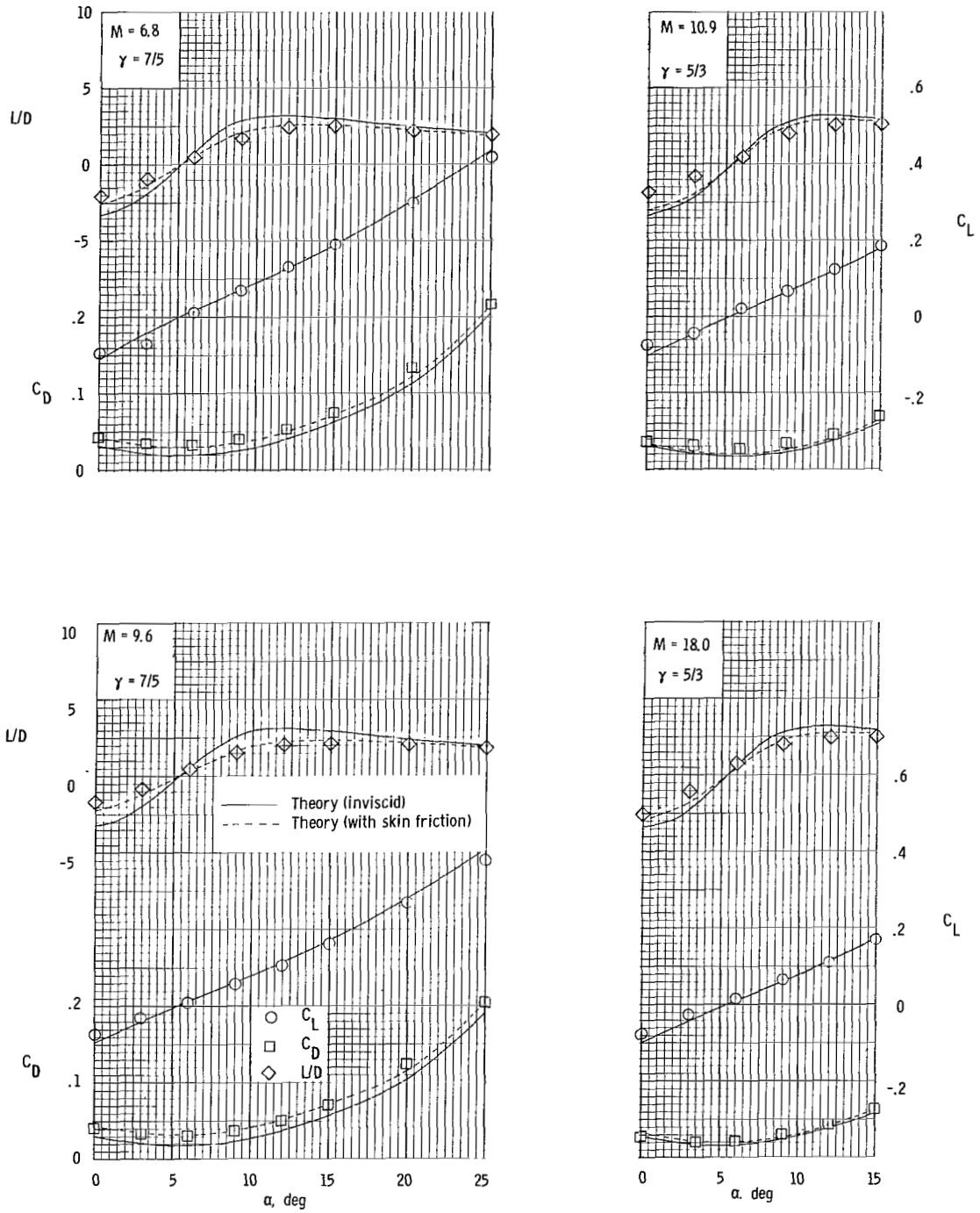

(g) $\Lambda = 60^\circ$ wing with blunt leading edge.

Figure 2.- Continued.

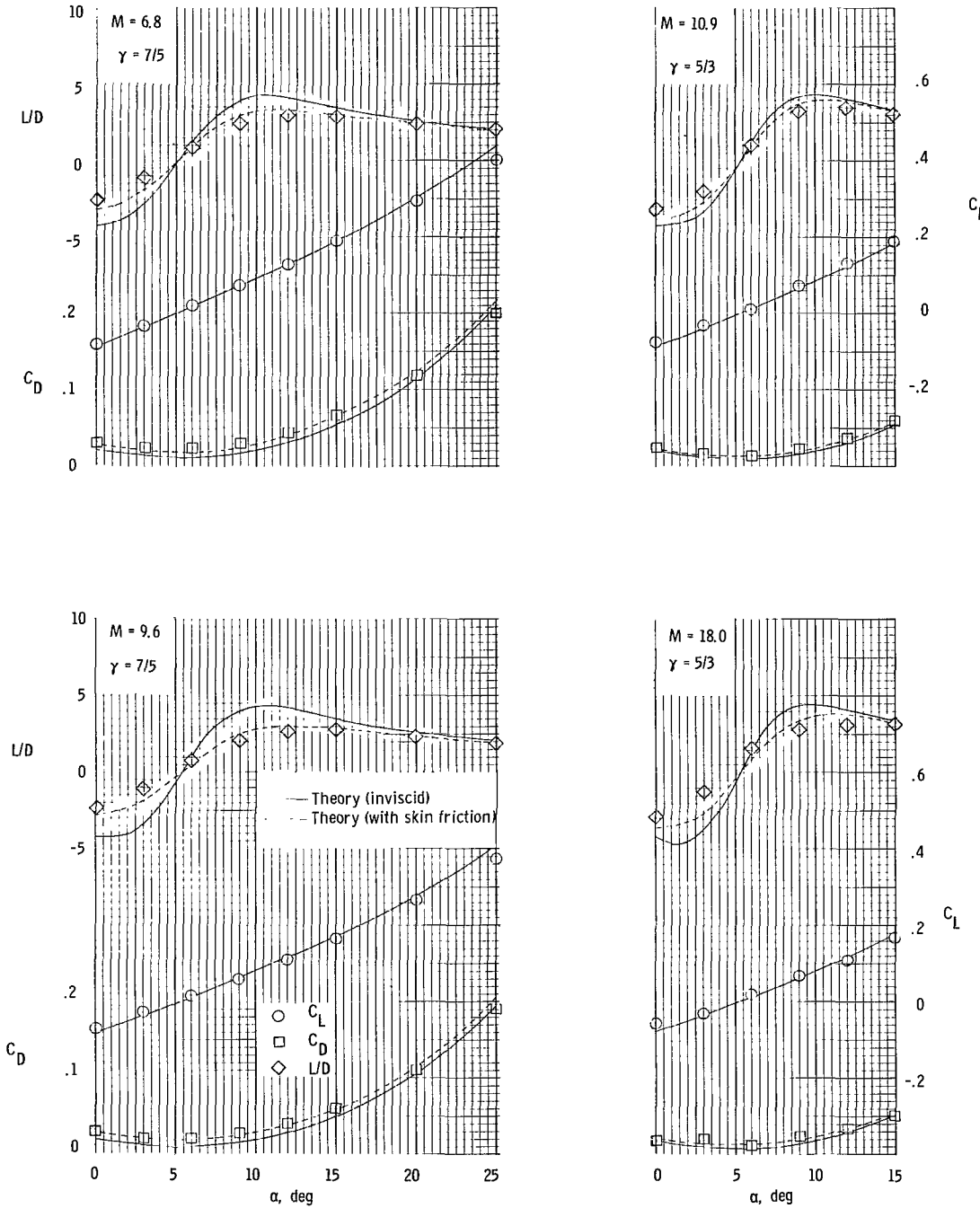

(h) $\Lambda = 70^{\circ}$ wing with blunt leading edge.

Figure 2.- Concluded.

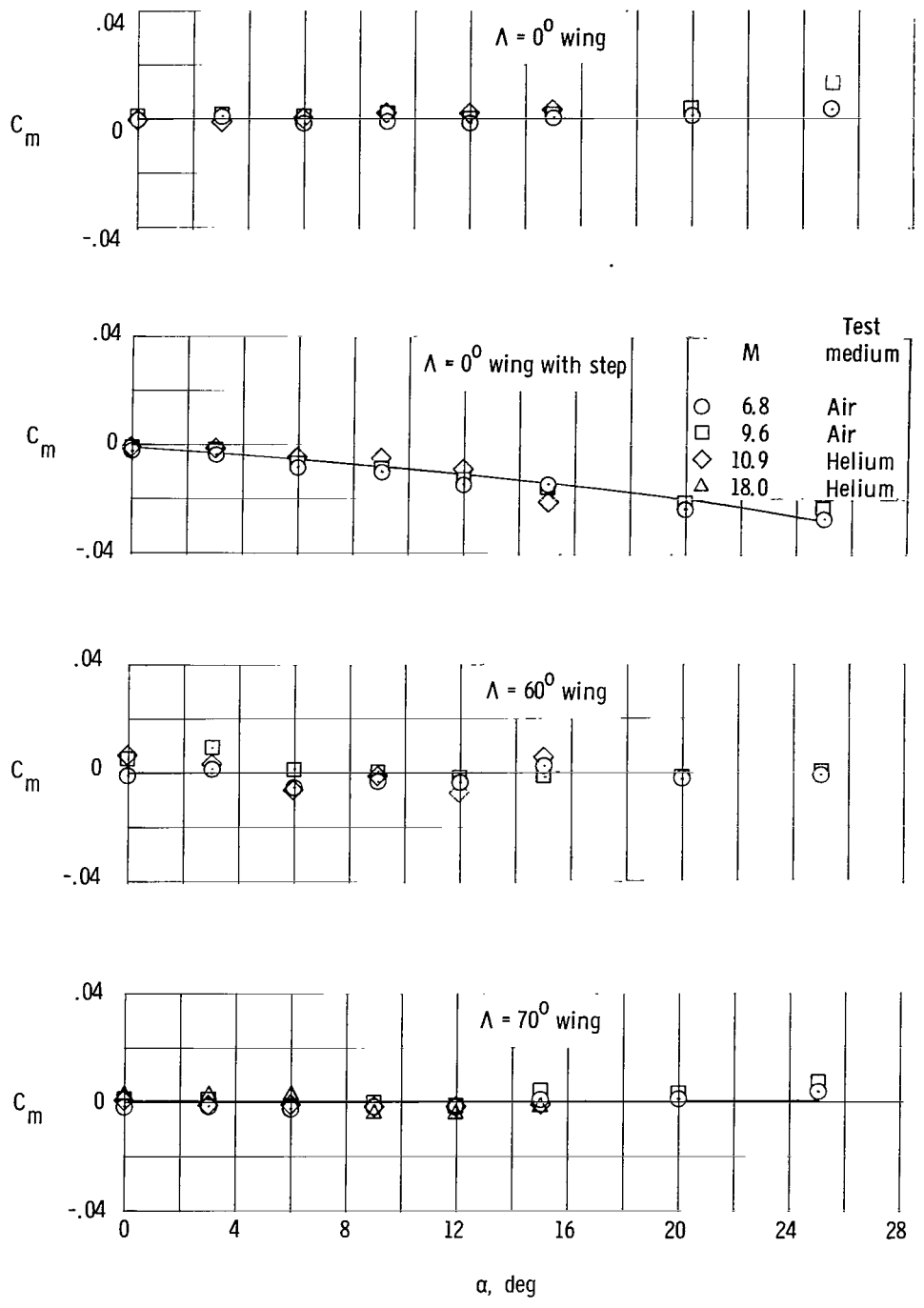

(a) Sharp-leading-edge wings.

Figure 3.- Pitching-moment coefficients plotted against angle of attack for the various wings.

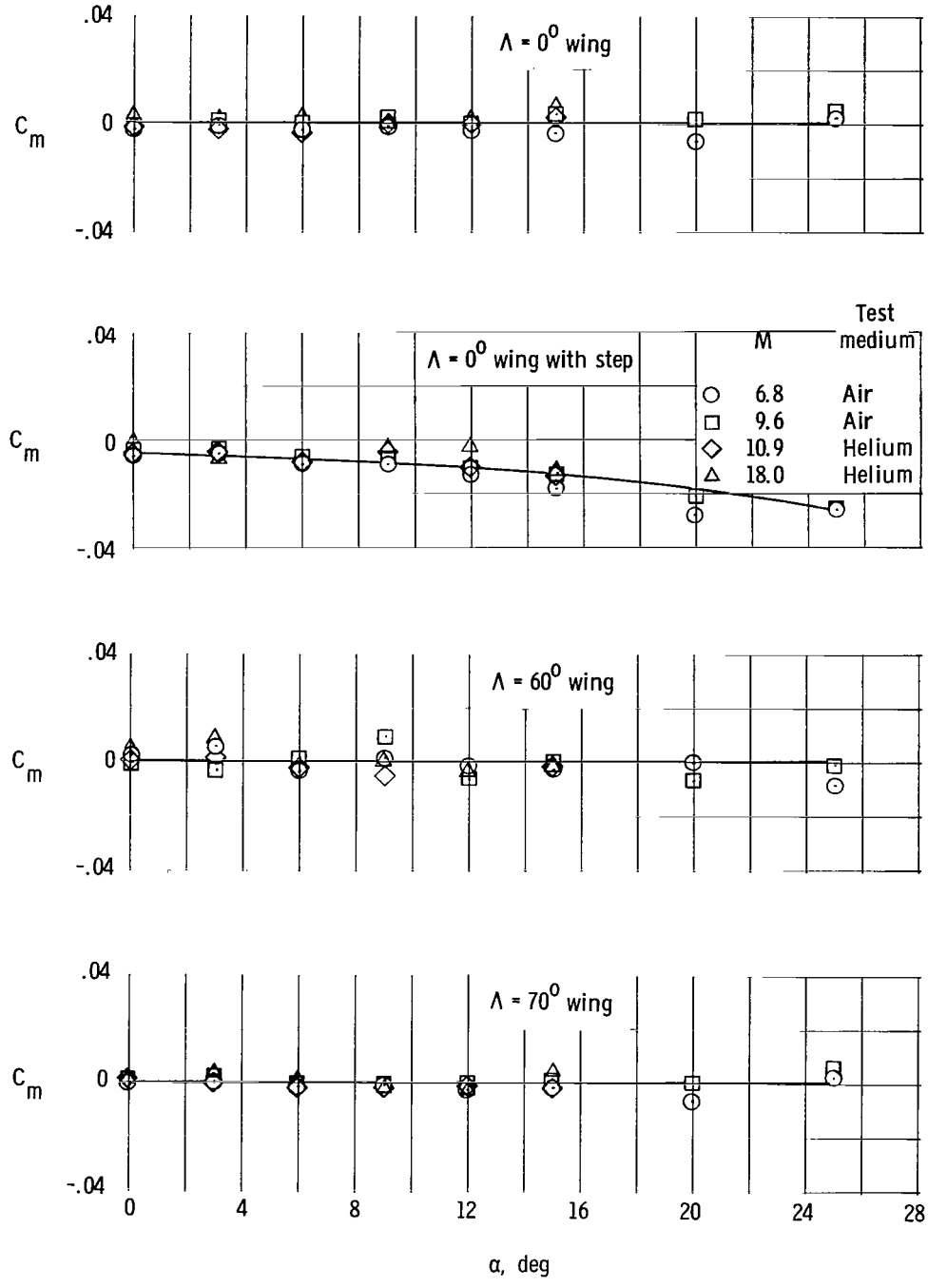

(b) Blunt-leading-edge wings.

Figure 3.- Concluded.

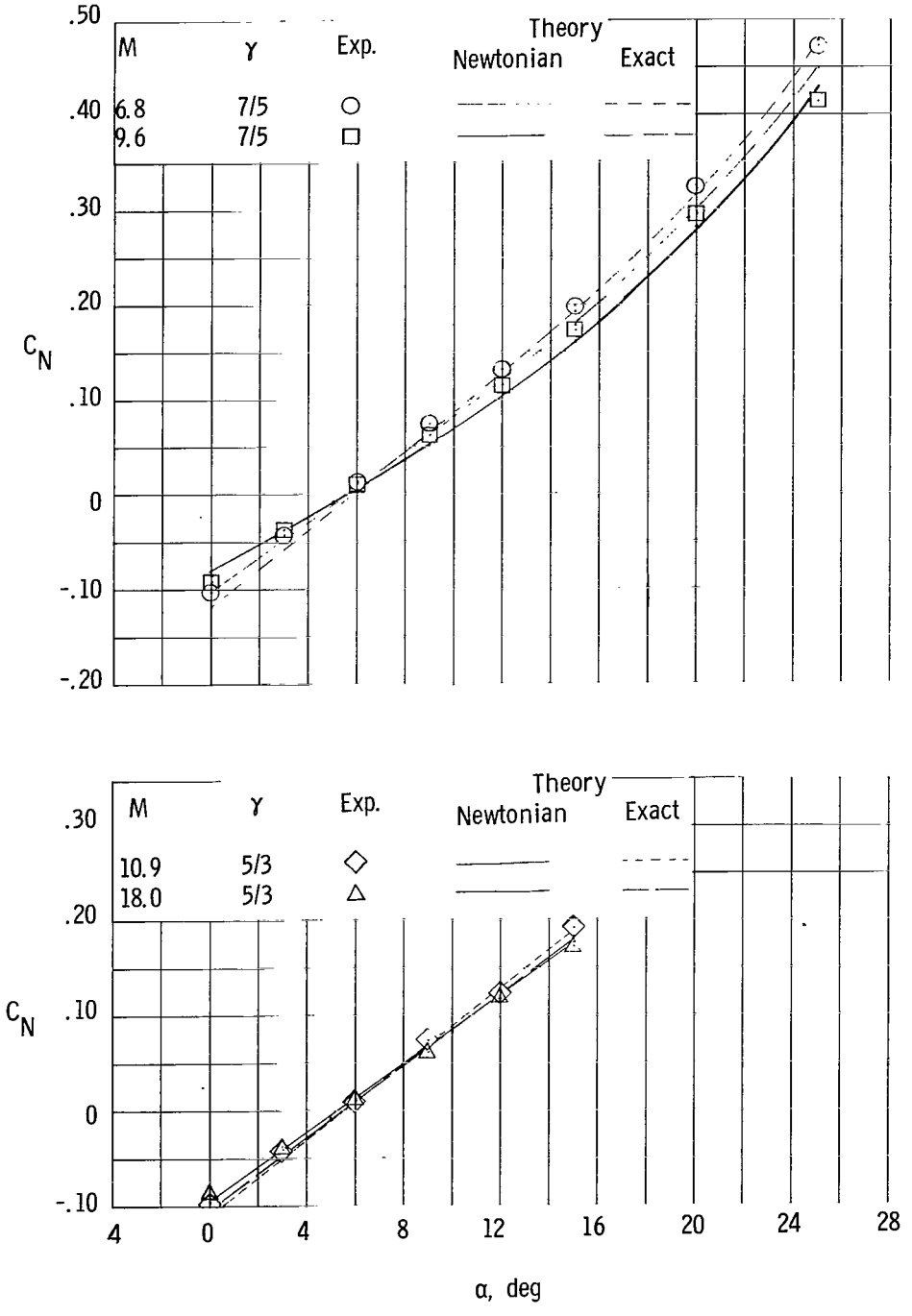

(a) $\Lambda = 0^\circ$ wing with sharp leading edge.

Figure 4.- A comparison of experimental normal-force coefficients with theory for the various wings.

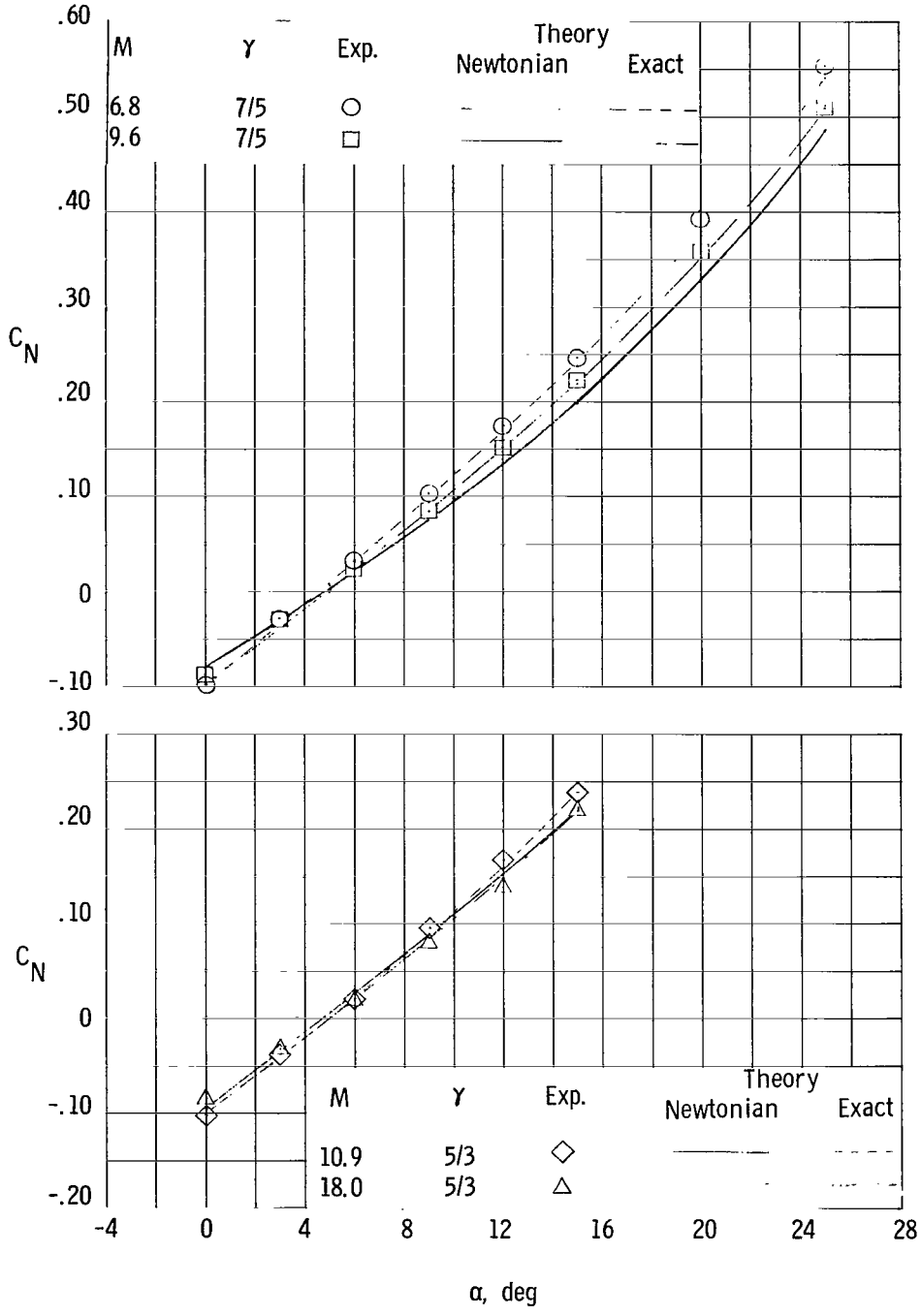

(b) $\Lambda = 0^{\circ}$ wing with sharp leading edge and forward-facing step.

Figure 4.- Continued.

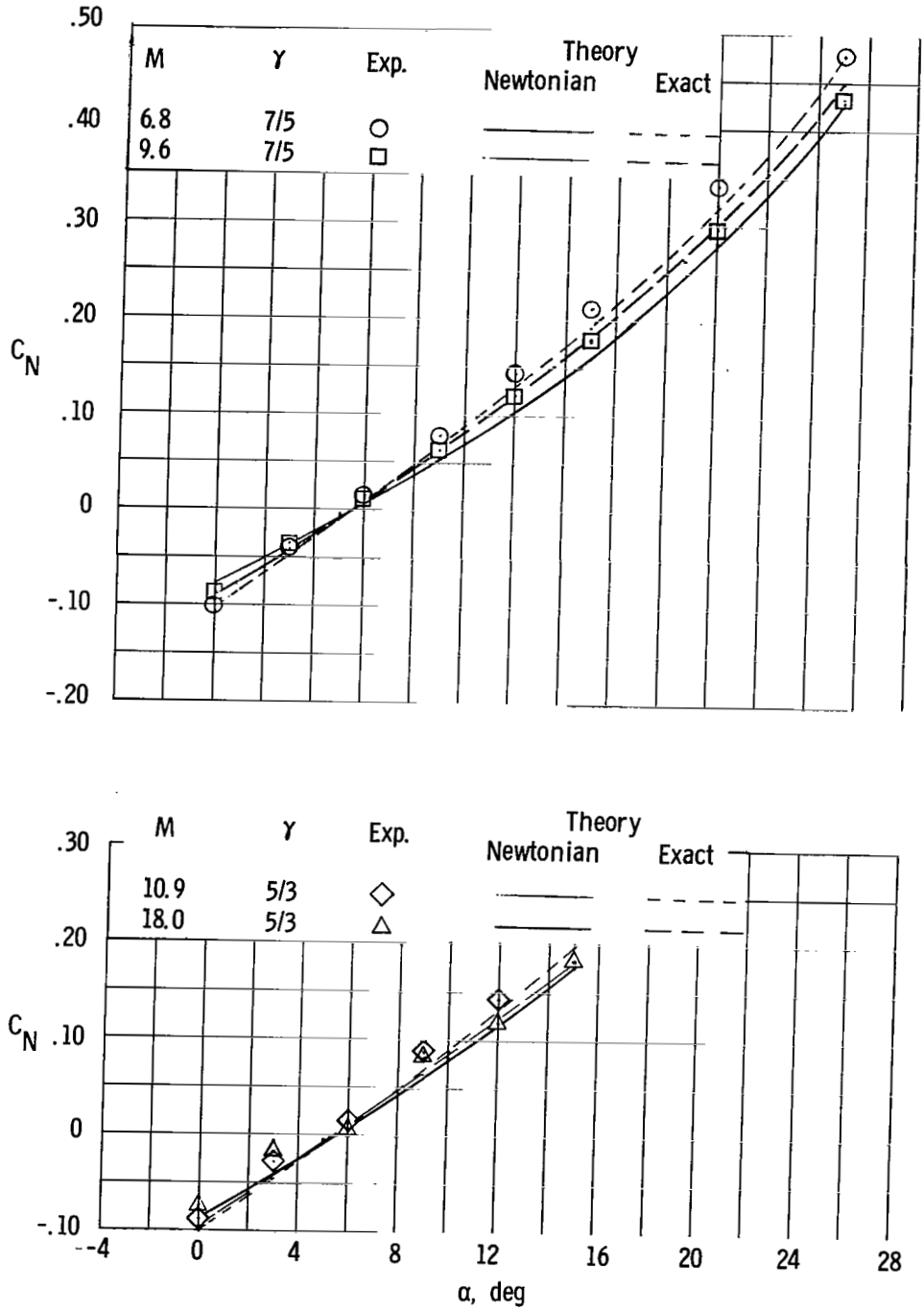

(c) $\Lambda = 60^\circ$ wing with sharp leading edge.

Figure 4.- Continued.

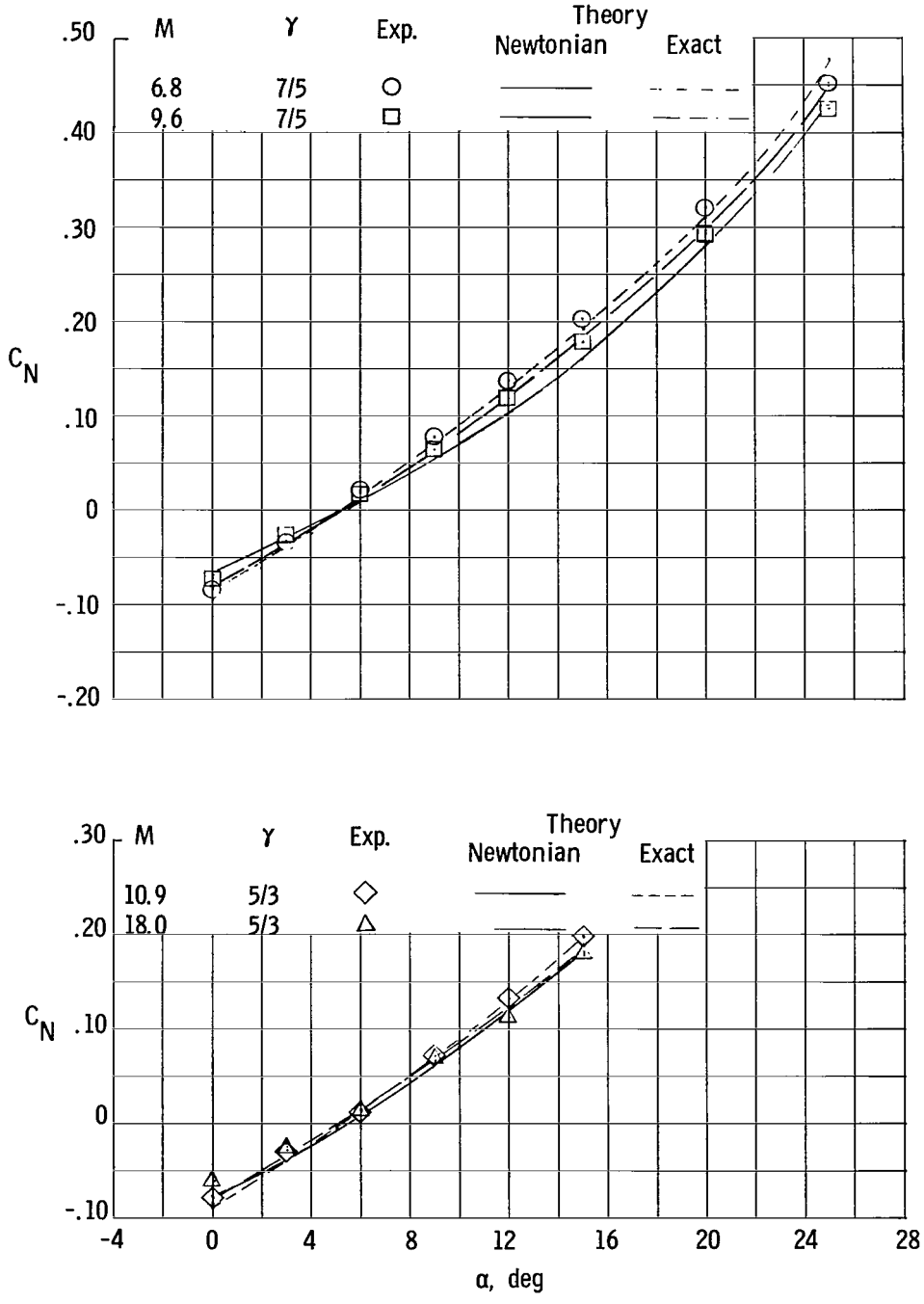

(d) $\Lambda = 70^\circ$ wing with sharp leading edge.

Figure 4.- Continued.

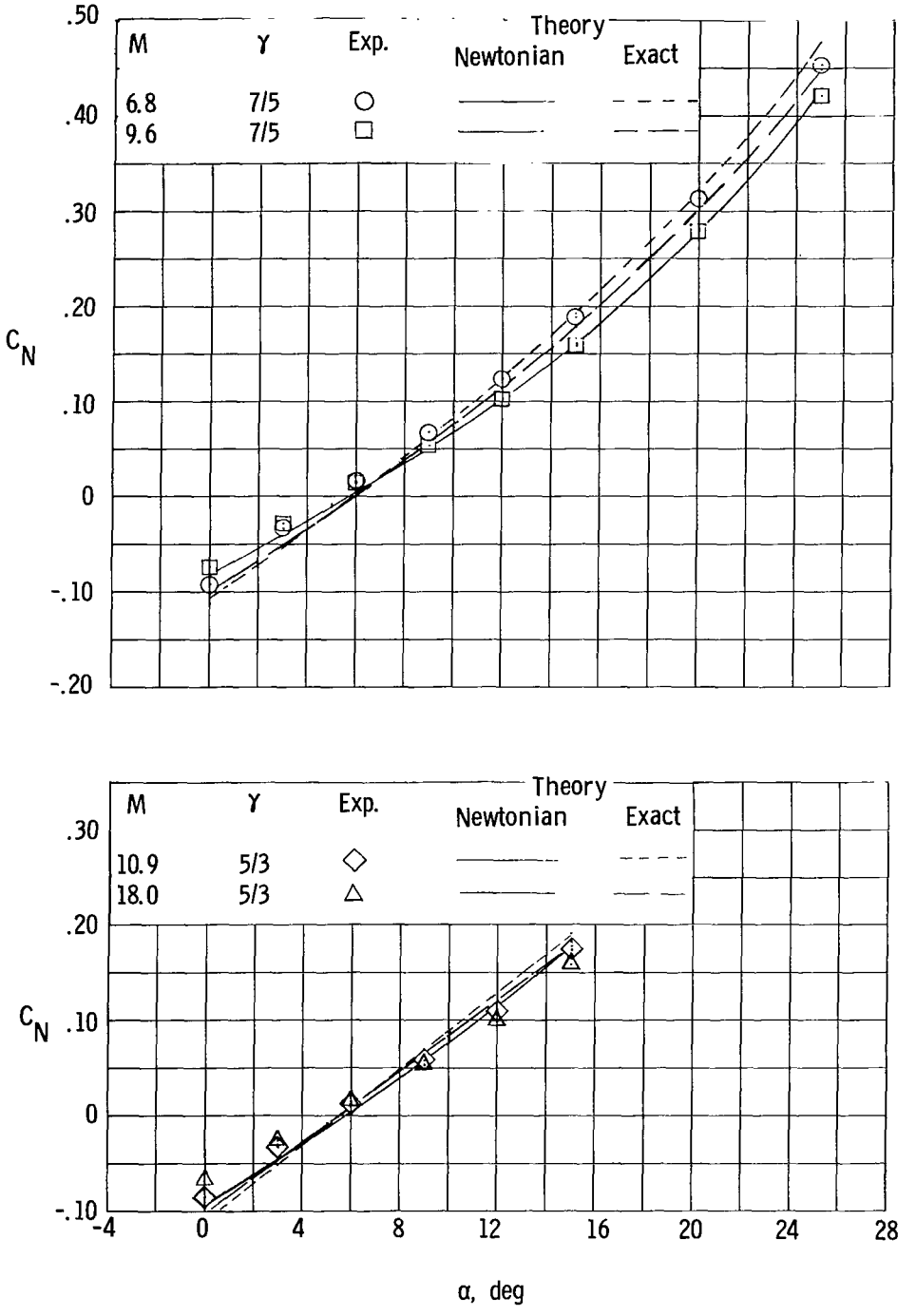

(e) $\Lambda = 0^\circ$ wing with blunt leading edge.

Figure 4.- Continued.

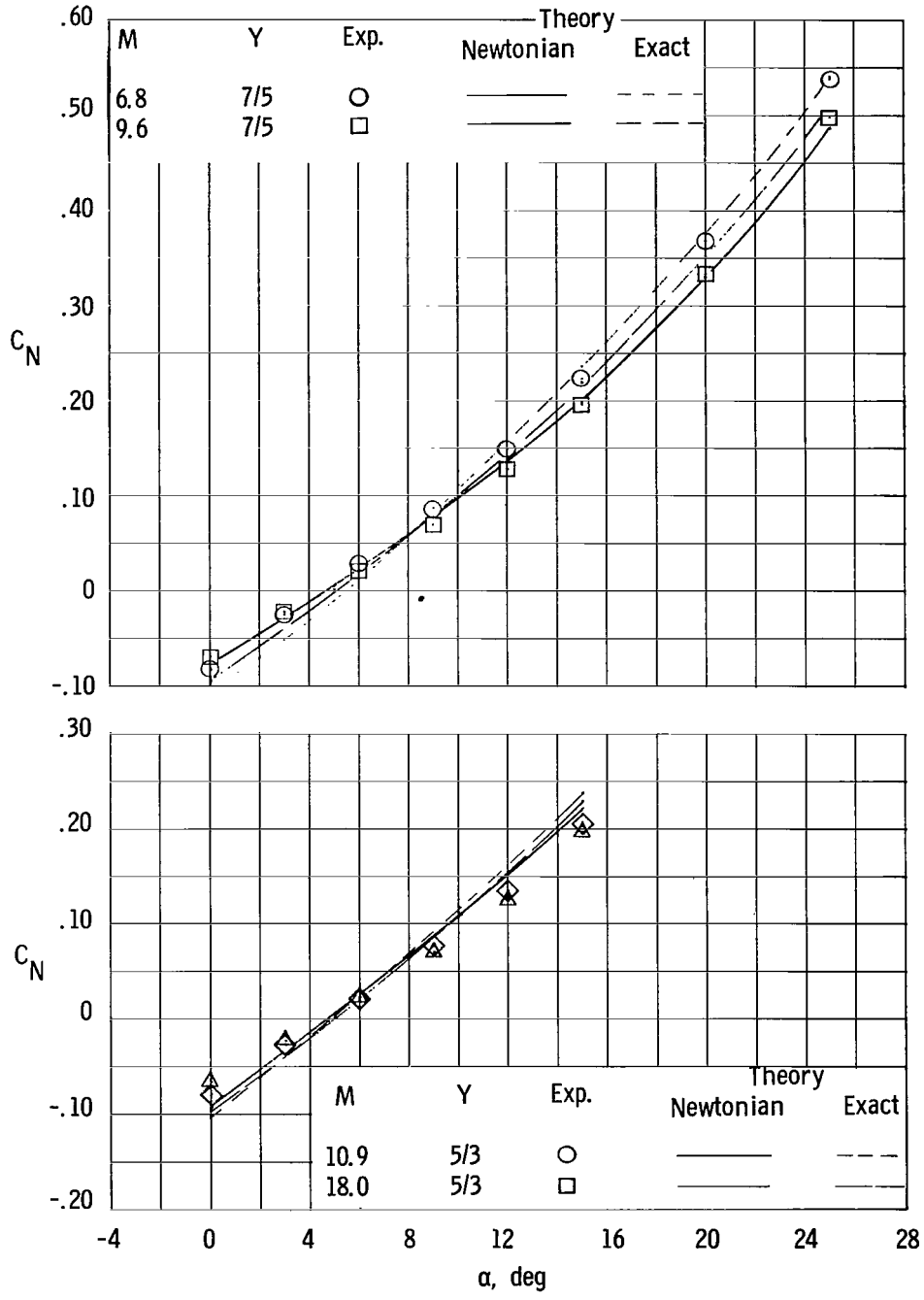

(f) $\Lambda = 0^{\circ}$ wing with blunt leading edge and forward-facing step.

Figure 4.- Continued.

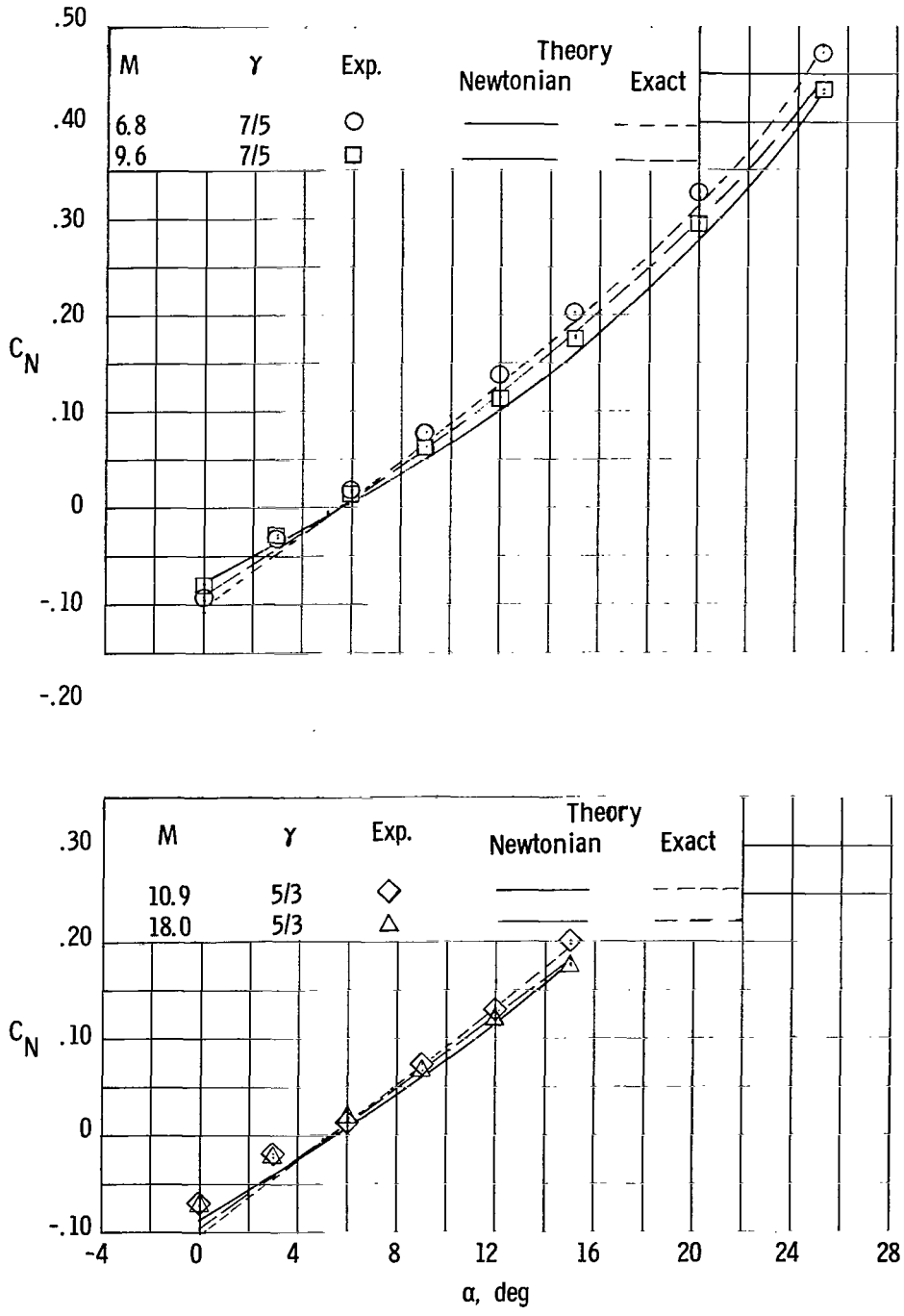

(g) $\Lambda = 60^\circ$ wing with blunt leading edge.

Figure 4.- Continued.

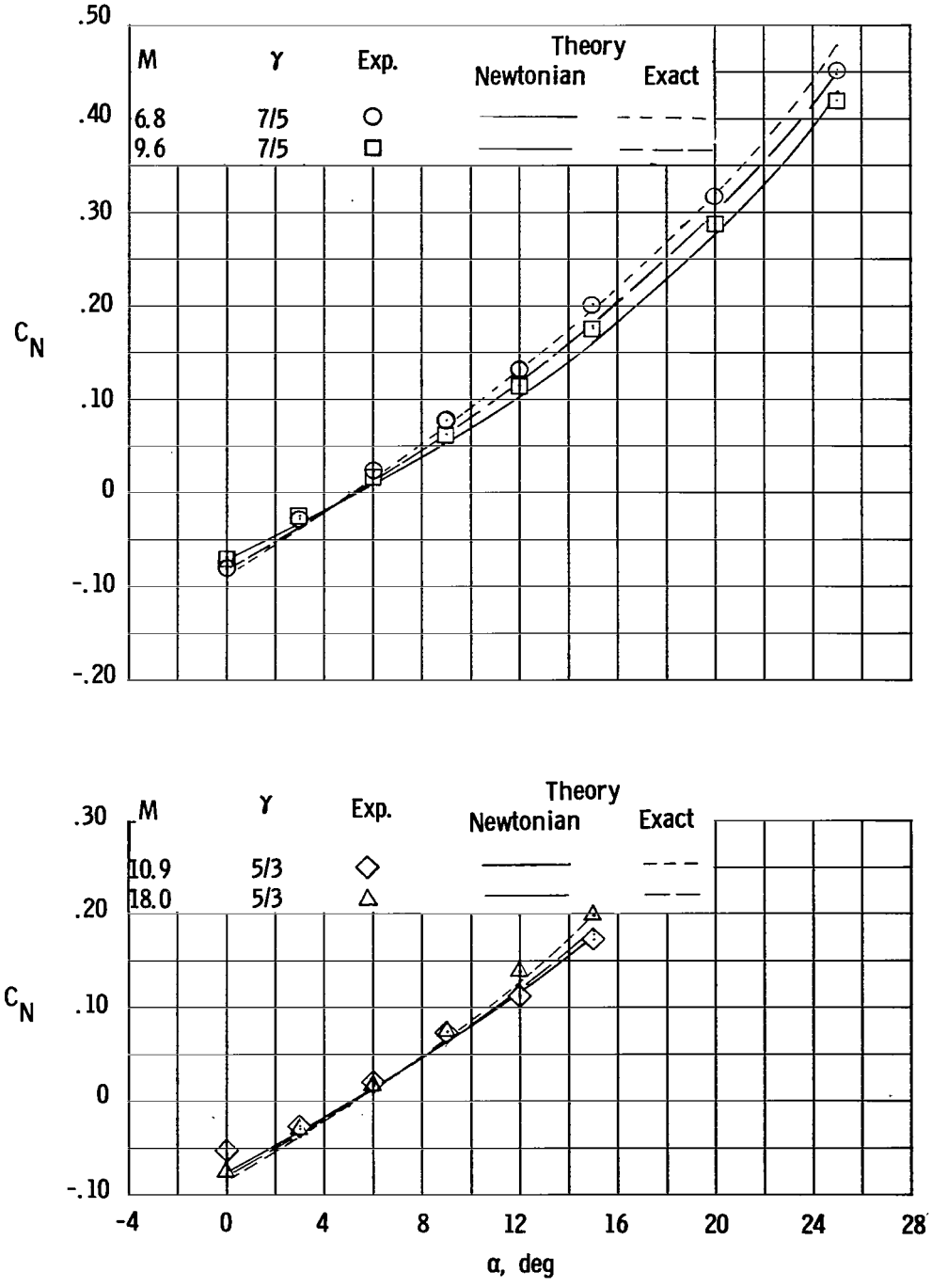

(h) $\Lambda = 70^{\circ}$ wing with blunt leading edge.

Figure 4.- Concluded.

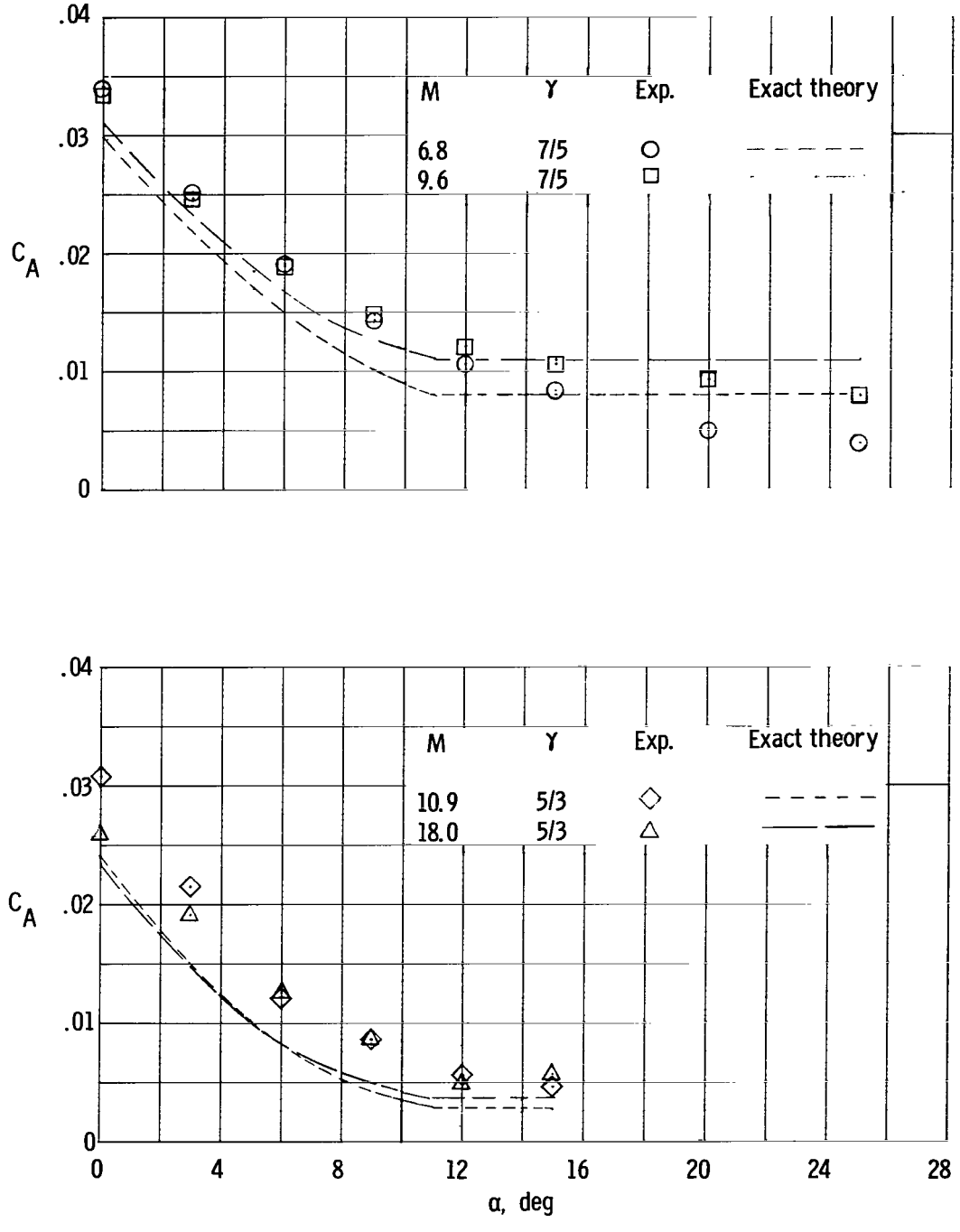

(a) $\Lambda = 0^{\circ}$ wing with sharp leading edge.

Figure 5.- A comparison of experimental axial-force coefficients with theory for the various wings.

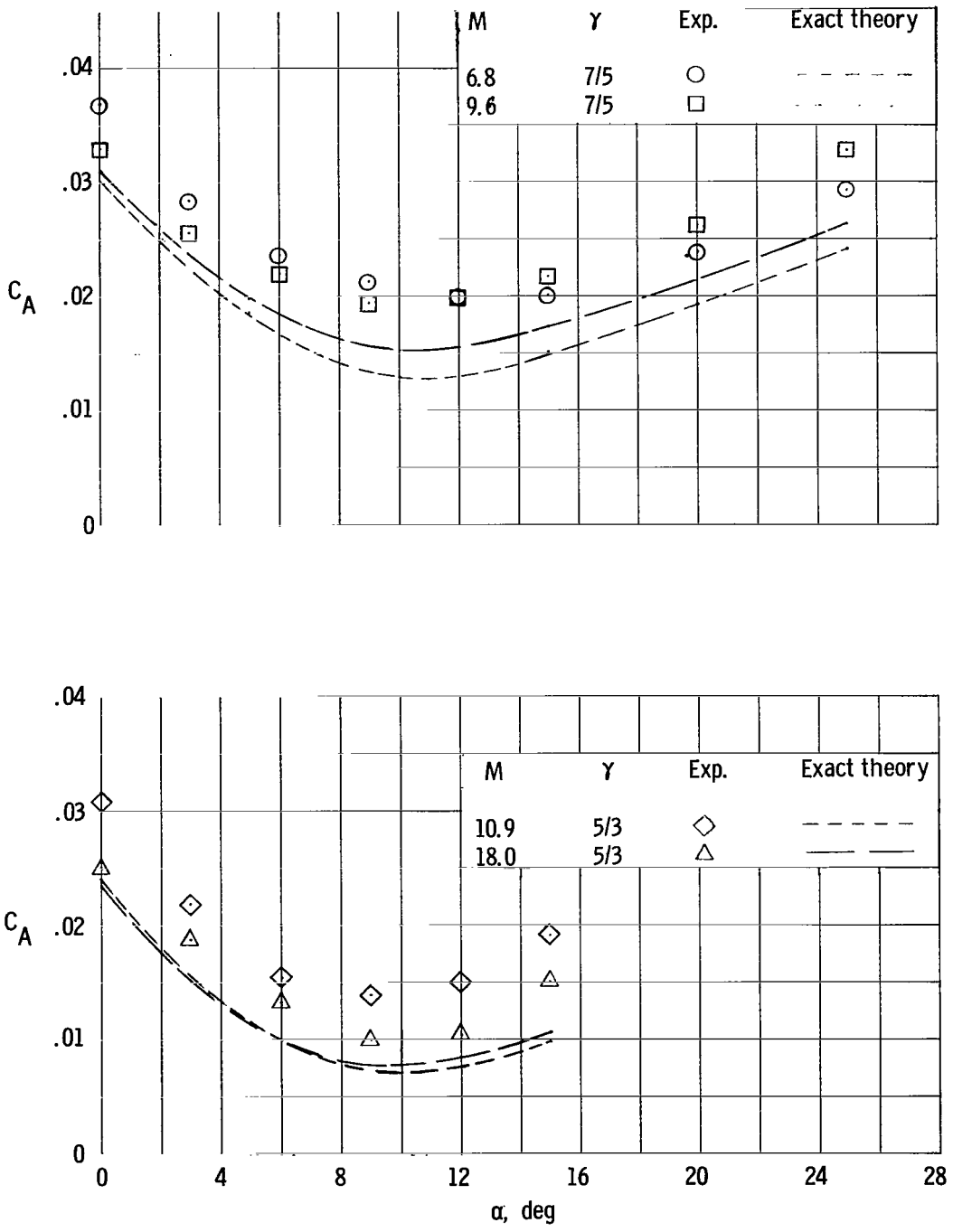

(b) $\Lambda = 0^\circ$ wing with sharp leading edge and forward-facing step.

Figure 5.- Continued.

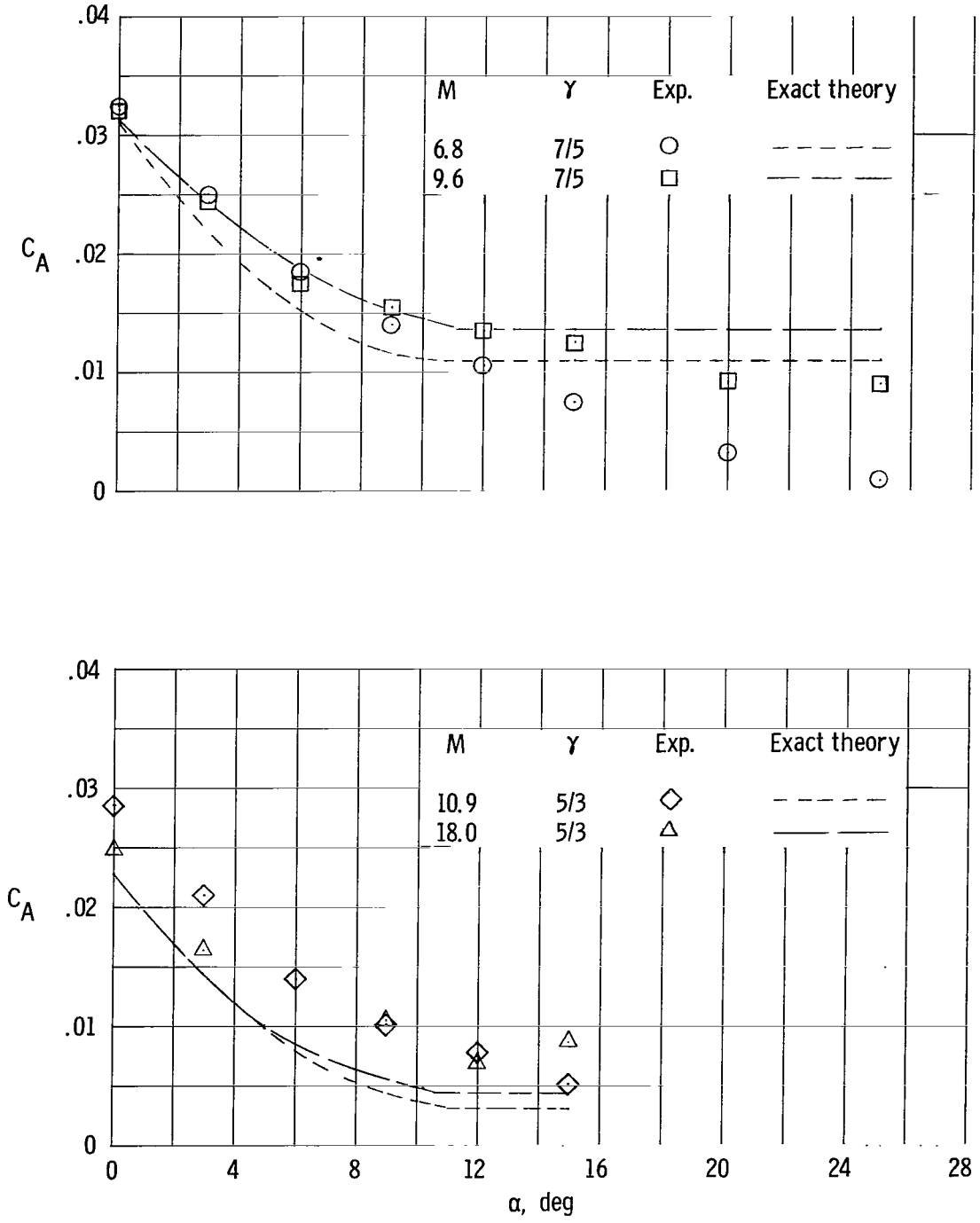

(c) $\Lambda = 60^\circ$ wing with sharp leading edge.

Figure 5.- Continued.

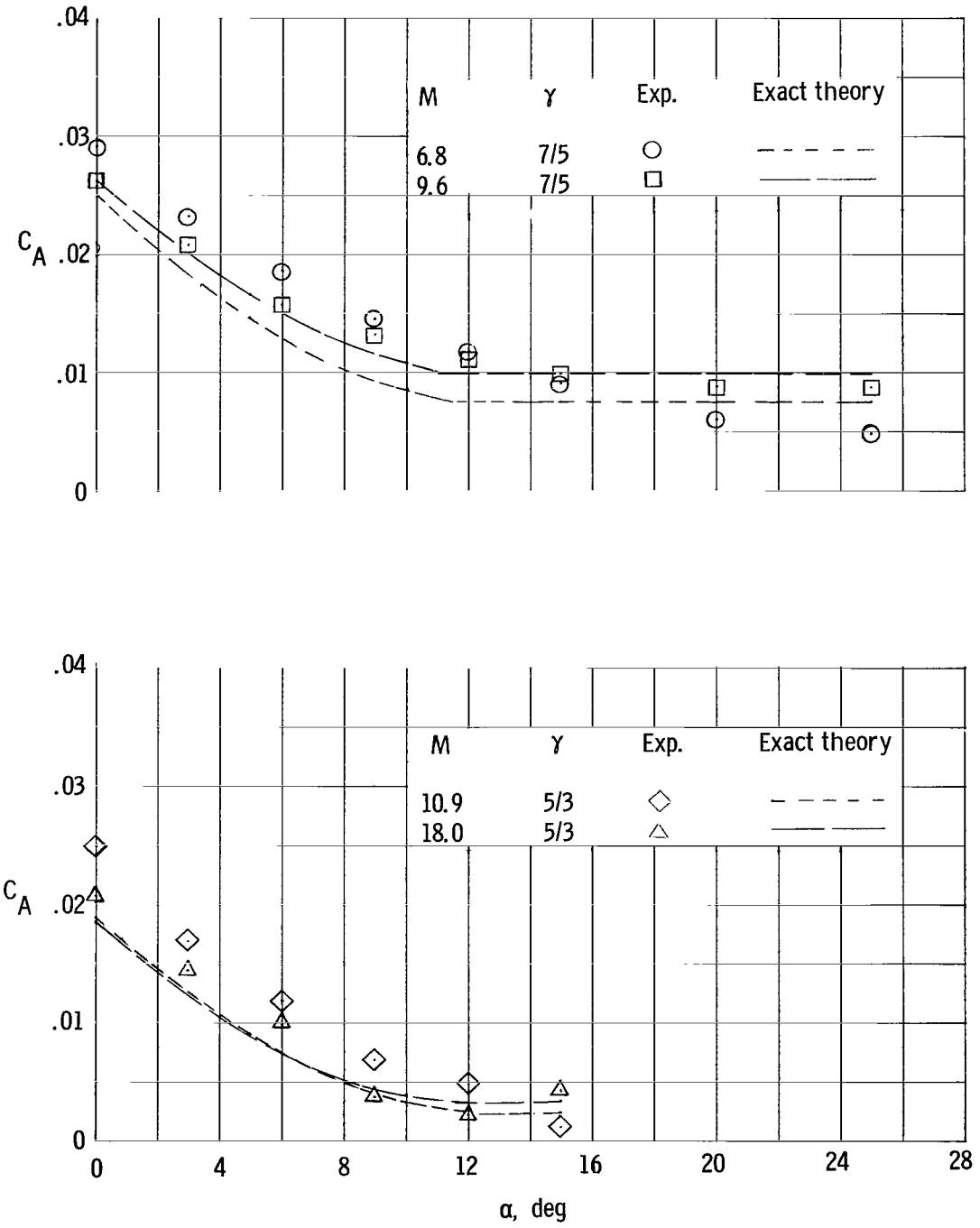

(d) $\Lambda = 70^\circ$ wing with sharp leading edge.

Figure 5.- Continued.

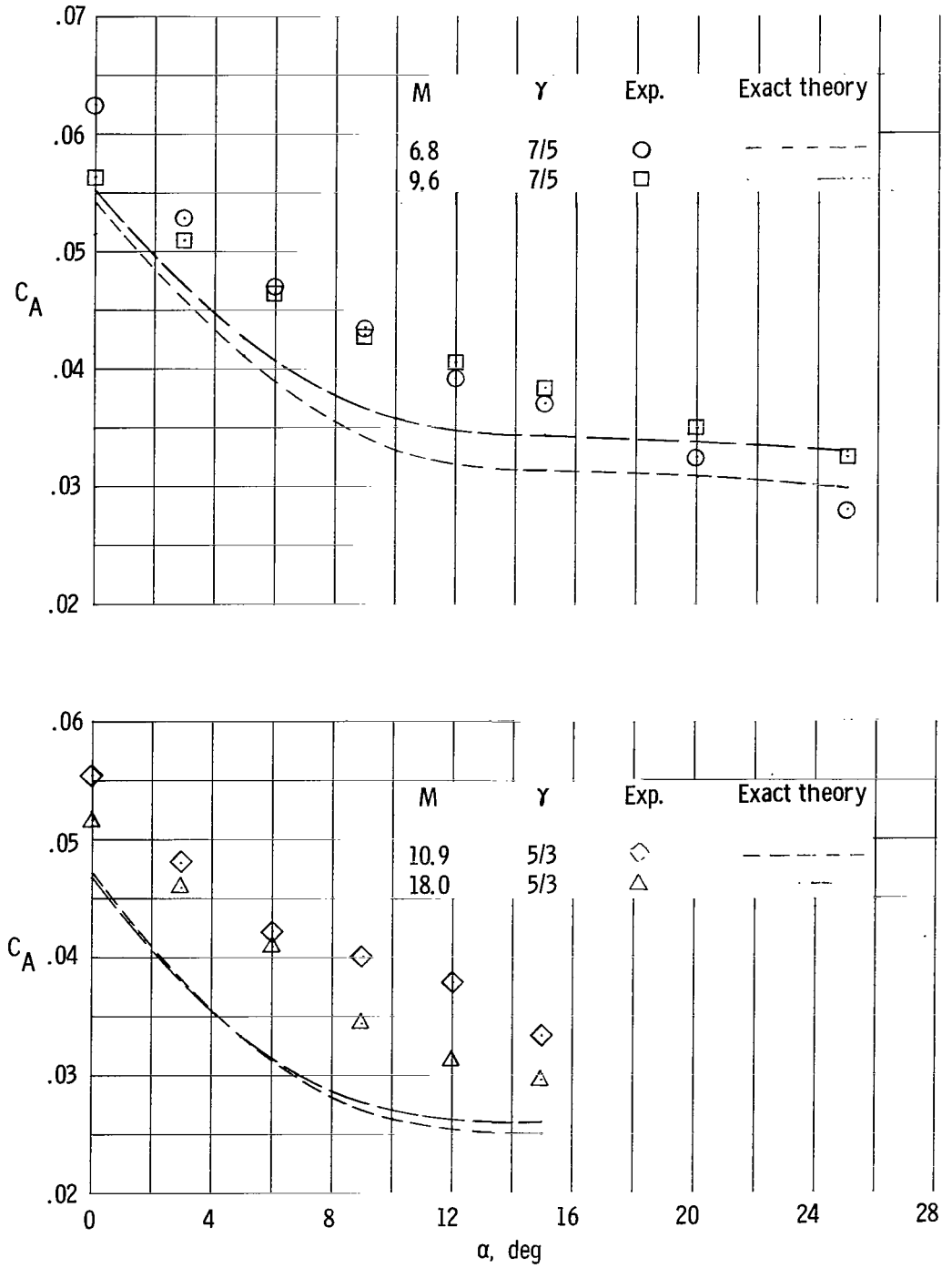

(e) $\Lambda = 0^{\circ}$ wing with blunt leading edge.

Figure 5.- Continued.

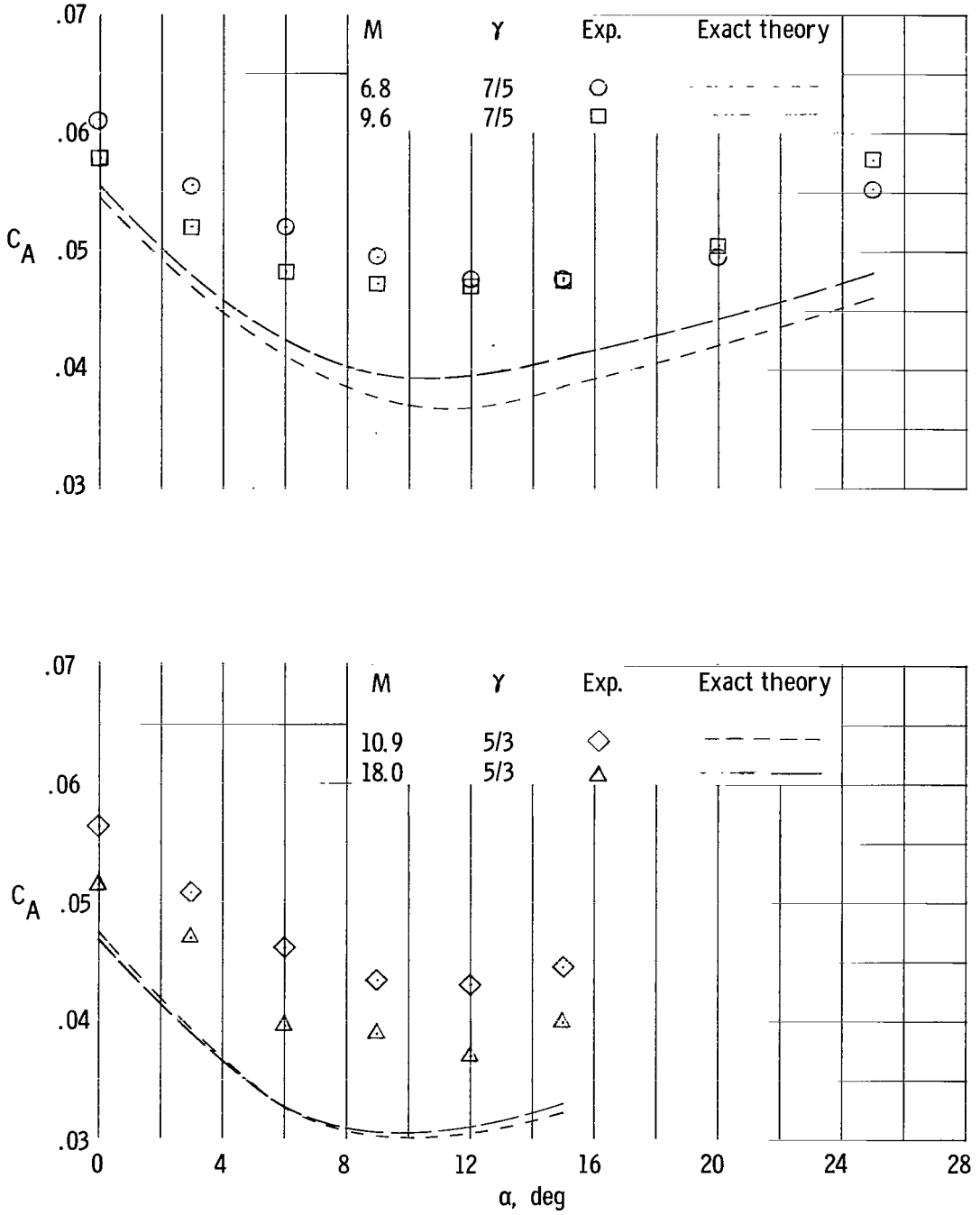

(f) $\Lambda = 0^\circ$ wing with blunt leading edge and forward-facing step.

Figure 5.- Continued.

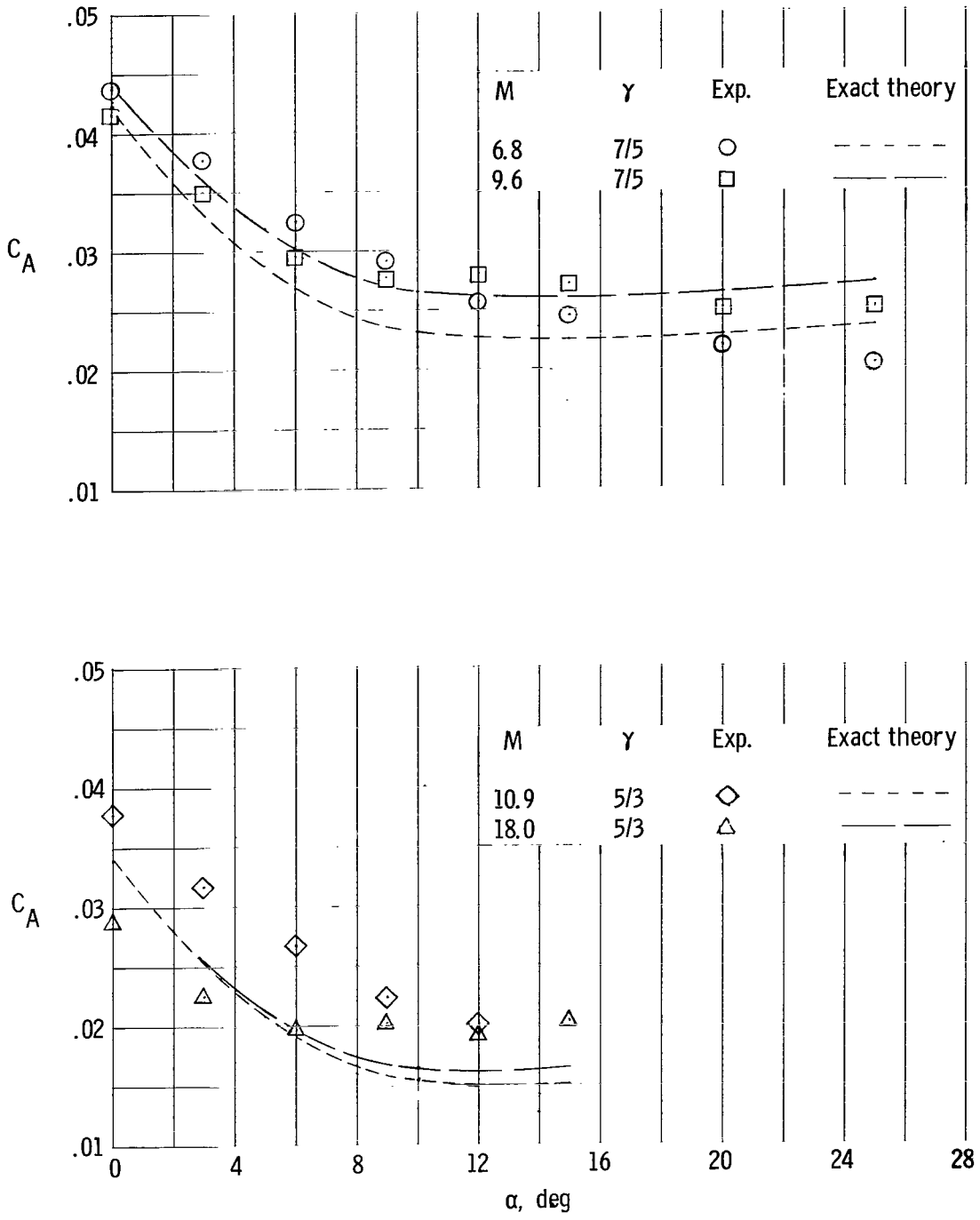

(g) $\Lambda = 60^\circ$ wing with blunt leading edge.

Figure 5.- Continued.

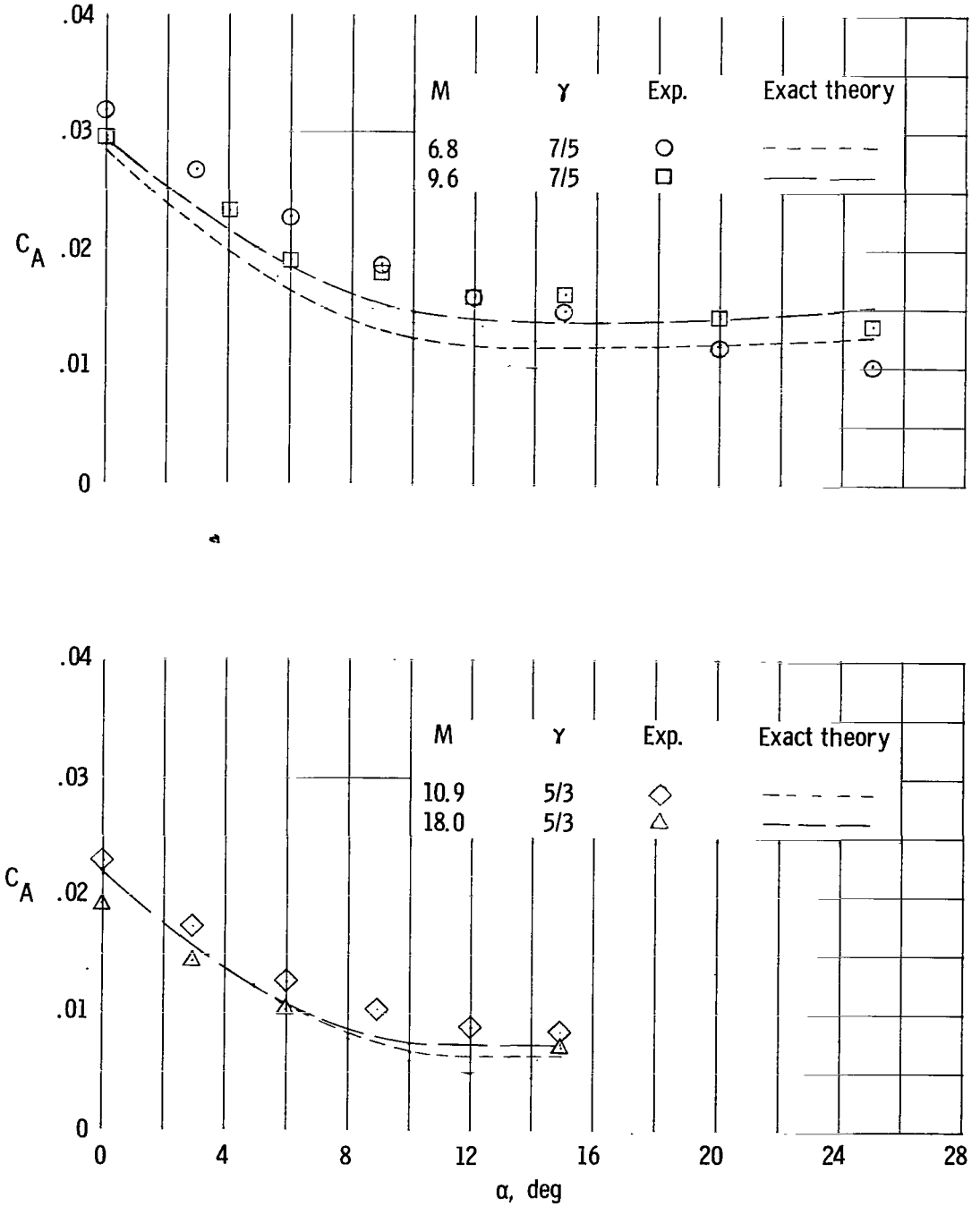

(h) $\Lambda = 70^{\circ}$ wing with blunt leading edge.

Figure 5.- Concluded.

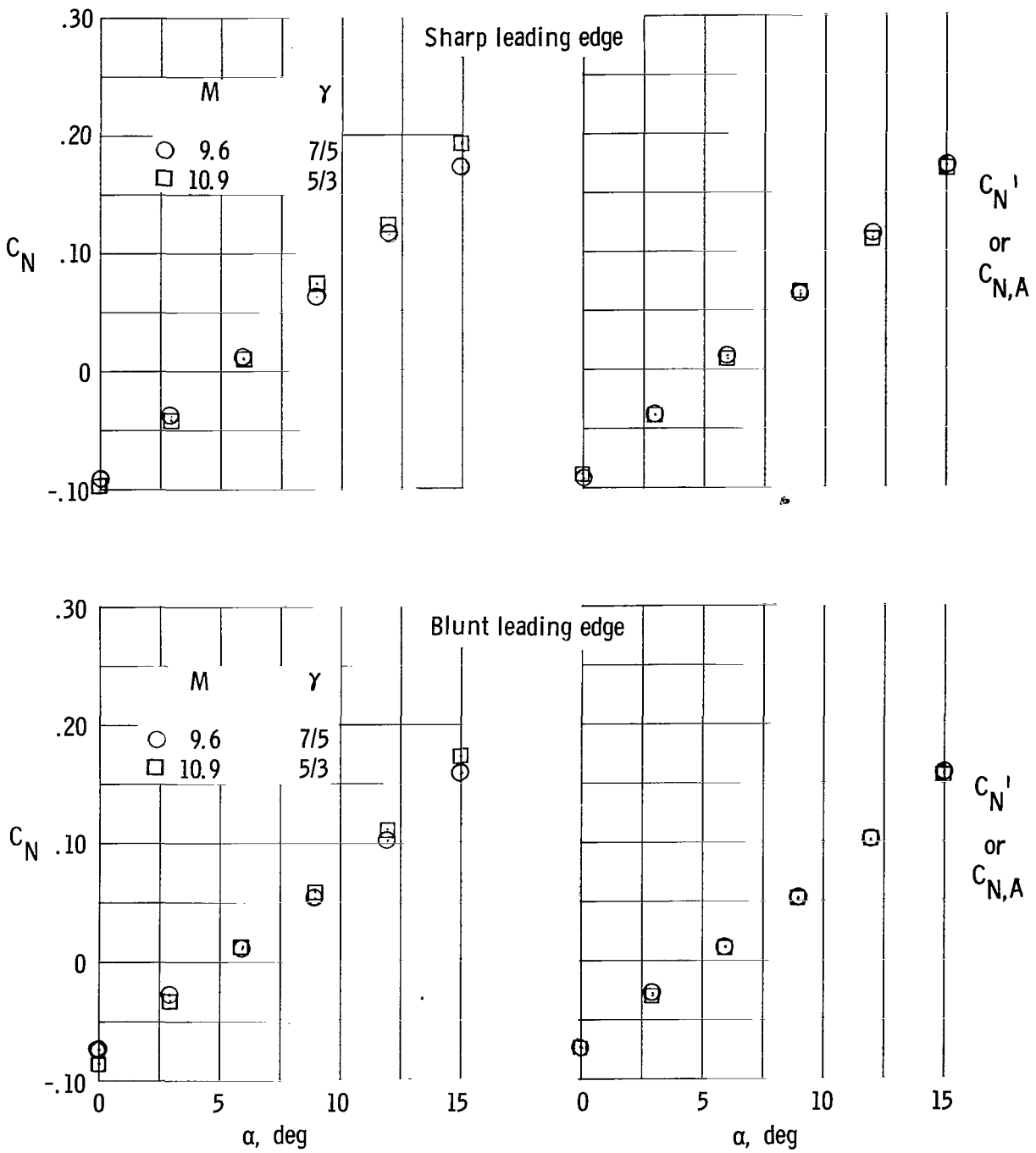

(a) $\Lambda = 0^\circ$ wing.

Figure 6.- Correlation by Newtonian method of normal-force coefficients for the various wings tested.

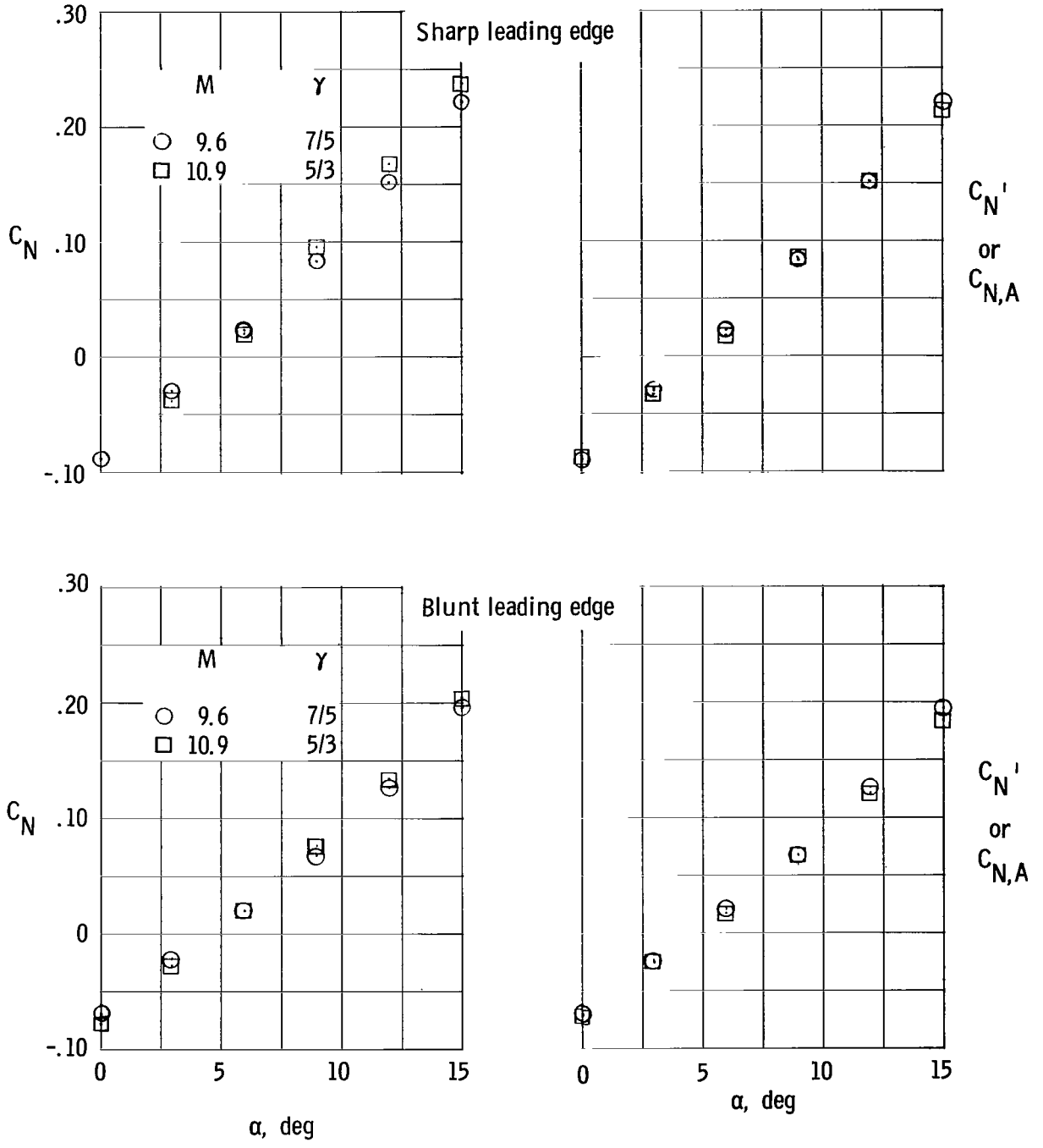

(b) $\Lambda = 0^{o}$ wing with forward-facing step.

Figure 6.- Continued.

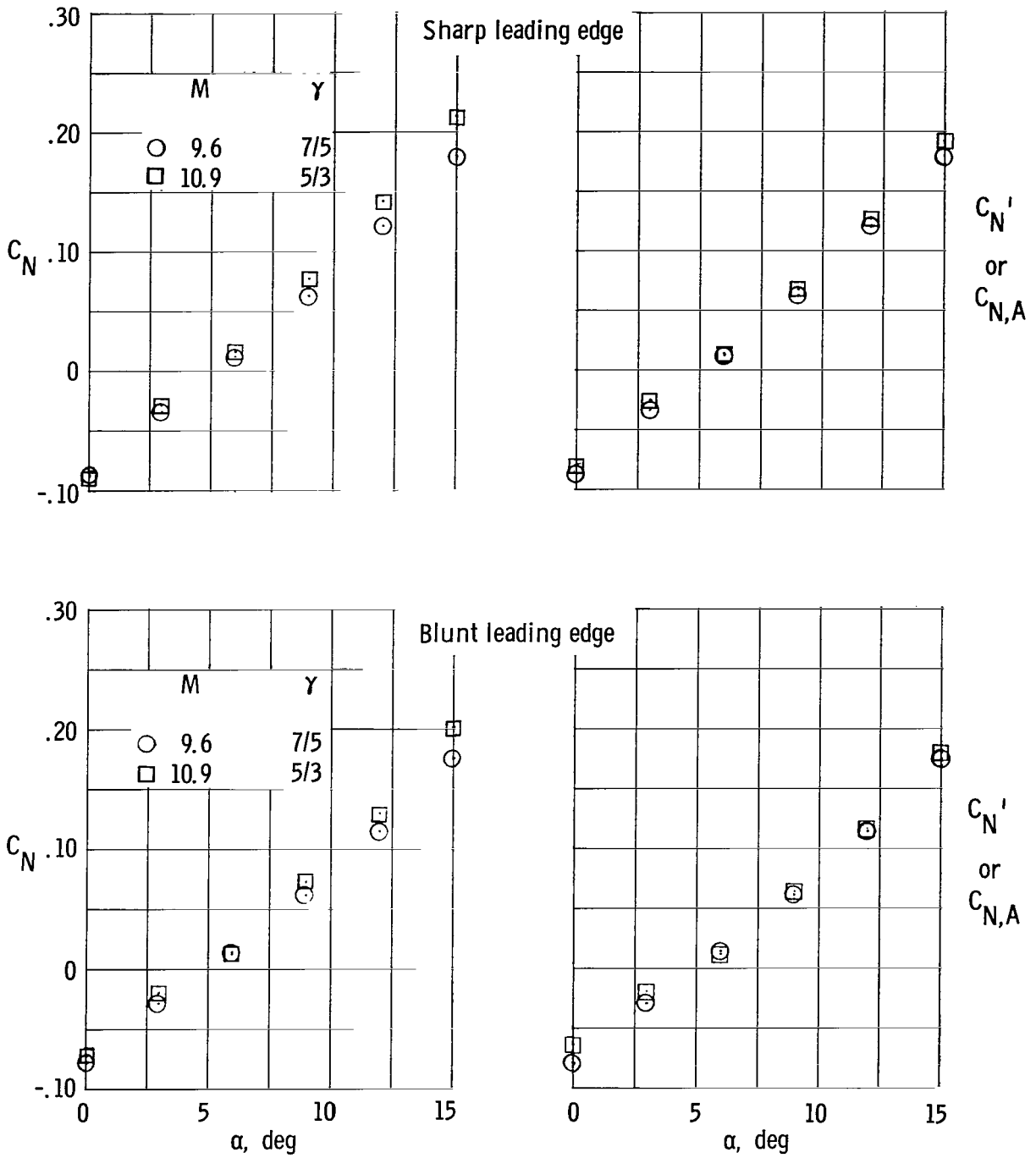

(c) $\Lambda = 60^\circ$ wing.

Figure 6.- Continued.

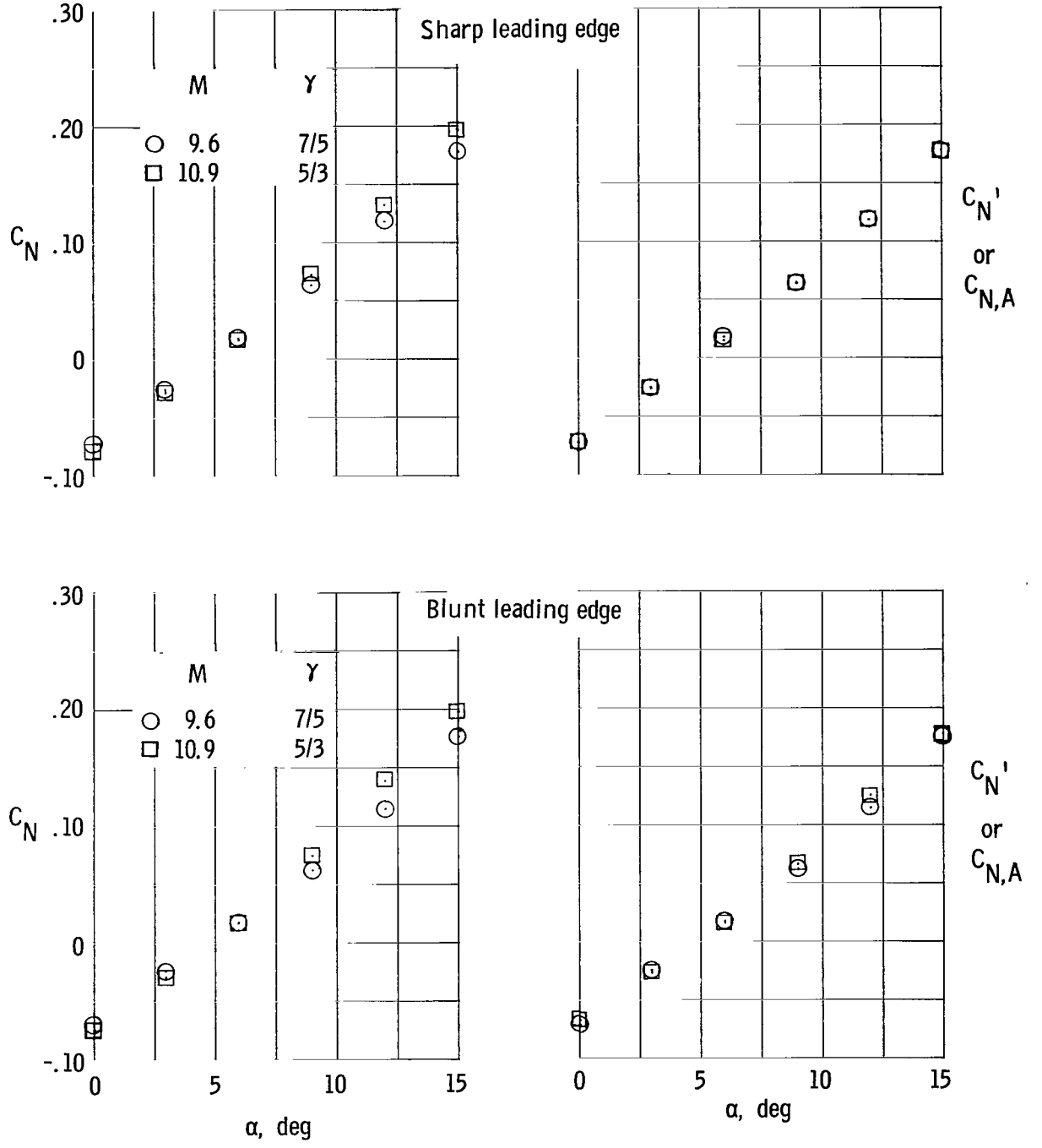

(d) $\Lambda = 70^{\circ}$ wing.

Figure 6.- Concluded.

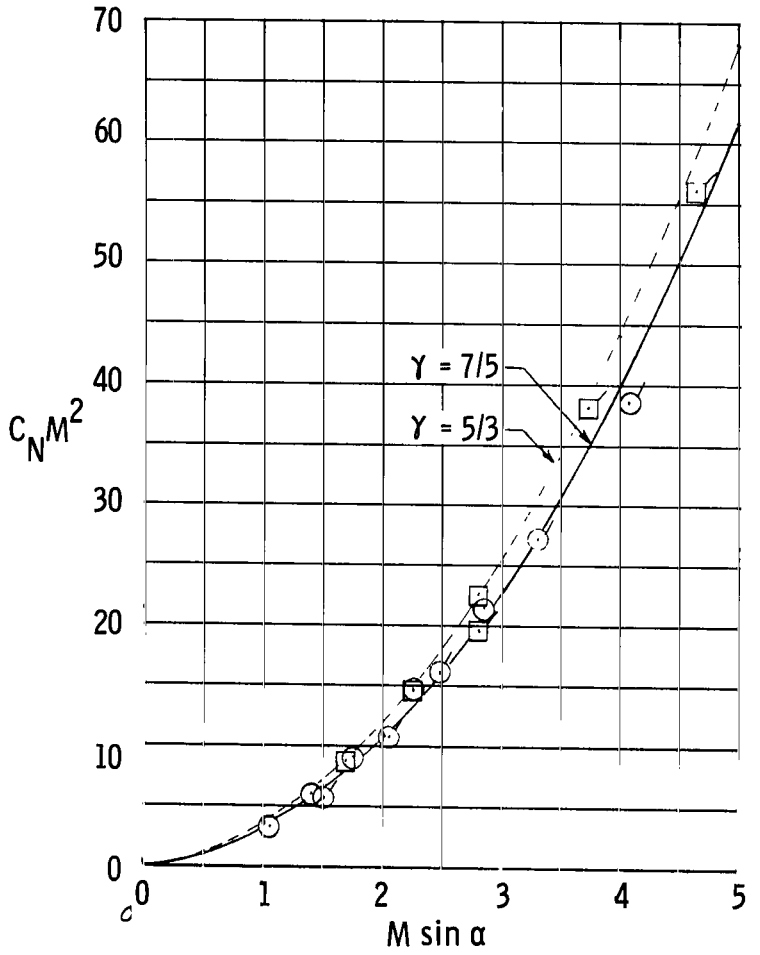

(a) Sharp leading edge.

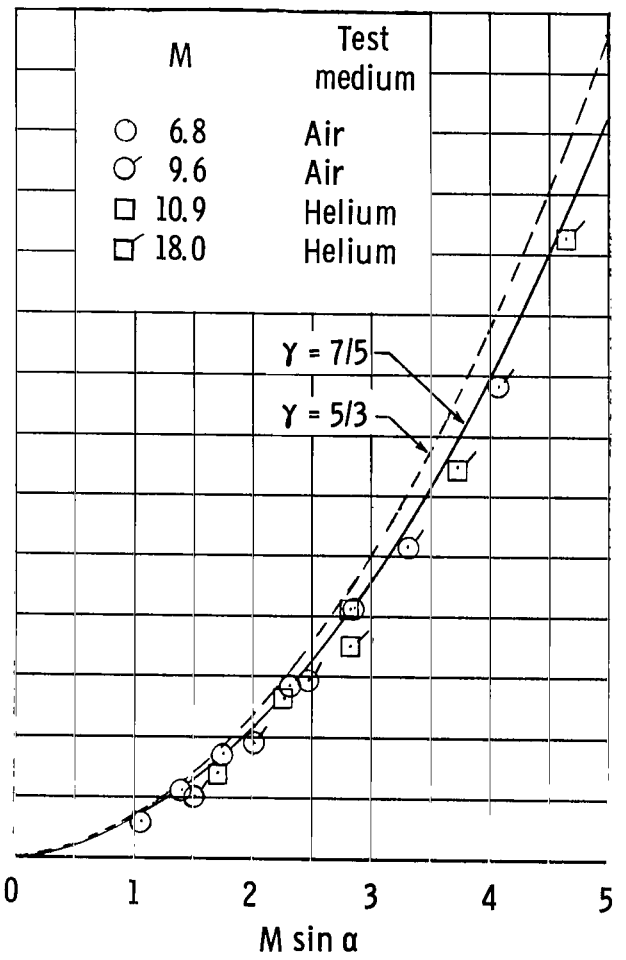

(b) Blunt leading edge.

Figure 7.- Correlation of normal-force coefficients for $\Lambda = 0^{\circ}$ wing.

2/7/85
ab

"The aeronautical and space activities of the United States shall be conducted so as to contribute . . . to the expansion of human knowledge of phenomena in the atmosphere and space. The Administration shall provide for the widest practicable and appropriate dissemination of information concerning its activities and the results thereof."

—NATIONAL AERONAUTICS AND SPACE ACT OF 1958

NASA SCIENTIFIC AND TECHNICAL PUBLICATIONS

TECHNICAL REPORTS: Scientific and technical information considered important, complete, and a lasting contribution to existing knowledge.

TECHNICAL NOTES: Information less broad in scope but nevertheless of importance as a contribution to existing knowledge.

TECHNICAL MEMORANDUMS: Information receiving limited distribution because of preliminary data, security classification, or other reasons.

CONTRACTOR REPORTS: Technical information generated in connection with a NASA contract or grant and released under NASA auspices.

TECHNICAL TRANSLATIONS: Information published in a foreign language considered to merit NASA distribution in English.

TECHNICAL REPRINTS: Information derived from NASA activities and initially published in the form of journal articles.

SPECIAL PUBLICATIONS: Information derived from or of value to NASA activities but not necessarily reporting the results of individual NASA-programmed scientific efforts. Publications include conference proceedings, monographs, data compilations, handbooks, sourcebooks, and special bibliographies.

Details on the availability of these publications may be obtained from:

SCIENTIFIC AND TECHNICAL INFORMATION DIVISION

NATIONAL AERONAUTICS AND SPACE ADMINISTRATION

Washington, D.C. 20546